Mon. Not. R. Astron. Soc. **000**, 000–000 (2001)

Spectropolarimetry of a Complete Infrared Selected Sample of Seyfert 2 Galaxies

S.L. Lumsden[1,2], C.A. Heisler[3], J.A. Bailey[2], J.H. Hough[4] and S. Young[4]
[1] Department of Physics and Astronomy, University of Leeds, Leeds LS2 9JT, UK
Email – sll@ast.leeds.ac.uk
[2] Anglo-Australian Observatory, PO Box 296, Epping, NSW 1710, Australia
Email – jab@aaoepp.aao.gov.au
[3] Mount Stromlo and Siding Spring Observatories, Private Bag, Weston Creek P.O., Weston, ACT 2611, Australia⋆
[4] Department of Physical Sciences, University of Hertfordshire, Hatfield, Hertfordshire, AL10 9AB, UK
Email – jhh@star.herts.ac.uk, sy@star.herts.ac.uk

15 June 2001

ABSTRACT
We report the results of a spectropolarimetric survey of a complete far infrared selected sample of Seyfert 2 galaxies. We have found polarized broad Hα emission in one new source, NGC5995. In the sample as a whole, there is a clear tendency for galaxies in which we have detected broad Hα in polarized light to have warm mid–far infrared colours ($F_{60\mu m}/F_{25\mu m} \lesssim 4$), in agreement with our previous results. However, a comparison of the optical, radio and hard x-ray properties of these systems leads us to conclude that this is a secondary consequence of the true mechanism governing our ability to see scattered light from the broad line region. We find a strong trend for galaxies showing such emission to lie above a critical value of the relative luminosity of the active core to the host galaxy (as measured from the [OIII] 5007Å equivalent width) which varies as a function of the obscuring column density as measured from hard x-ray observations. The warmth of the infrared colours is then largely due to a combination of the luminosity of the active core, the obscuring column and the relative importance of the host galaxy in powering the far infrared emission, and not solely orientation as we inferred in our previous paper. Our data may also provide an explanation as to why the most highly polarized galaxies, which appear to have tori that are largely edge-on, are also the most luminous and have the most easily detectable scattered broad Hα.

Key words: galaxies: Seyfert - galaxies: active - polarization - scattering - infrared: galaxies - X-rays: galaxies

1 INTRODUCTION

In the standard model for active galaxies (hereafter AGN), hard continuum radiation from the accretion disk around a massive black hole ionises the surrounding gas, which can be divided into two components: the broad line region (BLR) and the narrow line region (NLR), at distances from the core of $<$ 1pc and $<$ 1kpc, respectively (cf Osterbrock 1993). For the case of Seyfert galaxies, the classification into Seyfert 1 or 2 depends solely on the presence or absence of considerably broadened (several thousand kms^{-1}) permitted lines: ie, whether or not we can see the BLR in terms of the standard model. The simplest form of 'unification' for Seyfert galaxies invokes a dusty torus to obscure the light from the BLR in the Seyfert 2s, with the sole free parameter being inclination (see, for example, Antonucci 1993 for a review of unification schemes for Seyfert galaxies).

The firmest evidence in favour of this simple unified model comes from optical spectropolarimetry and x-ray spectroscopy. Spectropolarimetry reveals scattered broad permitted lines (eg. Antonucci and Miller 1985, Miller and Goodrich 1990). This can only come from a 'hidden' BLR (hereafter HBLR), that is obscured from our direct line of sight. Similarly, x-ray data for Seyfert 2s show evidence for either an absorbed Seyfert 1 like continuum in the hard x-ray band, or when the extinction is sufficiently large, a scattered spectrum characterised by an Fe Kα line with large equivalent width (see, for example, the recent summary of the results from the ASCA satellite by Turner et al. 1997a,b).

⋆ Charlene Heisler died after a long struggle with ill-health on October 28 1999. She will be greatly missed by all who knew her.

The evidence that at least some Seyfert 2s are in fact 'misaligned' Seyfert 1s is therefore compelling. However, previous samples in both the optical and x-ray have been selected in a fairly ad-hoc fashion. For the x-ray the limitation was simply sensitivity, so only the brightest x-ray sources, which also tend to be the least obscured, were studied. For the optical spectropolarimetry, sources were often initially chosen on the basis of their known high continuum polarization (eg. Miller and Goodrich 1990) or from *ad hoc* samples drawn from the literature (eg. Tran, Miller and Kay 1992, Kay 1994, Young et al. 1996a). In addition, with the exception of Kay (1994), who did not cover Hα in the spectral range of her data somewhat limiting its usefulness, and Young et al. (1996a), non-detections of HBLRs were rarely published.

Therefore it is not possible to use the published results on optical spectropolarimetry to test the unified model in a meaningful statistical sense, or, indeed, to determine if the simplest form of unification is actually the best match. In order to interpret whether the detection of an HBLR relates to orientation, or perhaps to other properties of the host galaxies, we must first understand how the initial galaxy sample is chosen. We therefore undertook a new survey in which we obtained optical spectropolarimetry of a sample with well understood far infrared properties. As discussed in Section 2, the far infrared luminosity is likely to be a relatively extinction (and hence orientation) independent measure of the combined AGN and host galaxy luminosity. In addition, there was a notable trend shown in early detections of HBLRs for those galaxies to have 'warm' mid–far infrared colours (eg Inglis et al. 1993). We therefore wished to determine if this was still true for a larger sample, and that the AGN with cooler colours did *not* show evidence for HBLRs. The initial results of that survey were reported in Heisler, Lumsden and Bailey (1997: hereafter Paper 1). There we reported an apparent trend for HBLRs to only appear in those AGN where $F_{60\mu m}/F_{25\mu m} < 4$. Since the mid-far infrared emission in Seyfert galaxies is dominated by thermal emission from dust, this trend is consistent with the unified model, since low values of the $F_{60\mu m}/F_{25\mu m}$ ratio imply warmer dust temperatures. Therefore we concluded that galaxies with warm mid-far infrared colours had tori that were closer to face-on, and hence more likely to show scattered radiation from the BLR.

However, our initial survey did suffer from some problems relating to the actual sample observed (see Section 2 for details), and was simply too small to test for other dependencies in the data that might mimic the effect that orientation would have. In particular, it is possible that star formation may play an increasingly important role in the AGN with cooler mid–far infrared colours, since the dust emission surrounding HII regions typically peaks nearer 100μm. Alexander (2001) suggested that the hard x-ray emission from the sample given in Paper 1 is consistent with such a picture, since the AGN with both warm and cool colours show a similar spread in implied neutral hydrogen column density. He inferred from this that the mid-far infrared colours related more to the presence or absence of significant star formation rather than orientation. In addition he noted, as had Tran et al. (1999), that there was an apparent trend for the HBLRs to have higher [OIII] 5007Å/Hβ ratios, and indeed for this ratio to be correlated with mid–far infrared colour. Again, this may be consistent with enhanced star formation in the galaxies with cooler colours, since the starburst will enhance Hβ but have relatively little effect on [OIII] emission in most cases.

This paper therefore presents the results of an extended survey of far infrared selected AGN. Since Paper 1 we have also refined our selection to exclude objects whose actual classification is in doubt (see Section 2.5). We will present the full spectropolarimetric data, including non-detections, for all objects for which we acquired data in a later paper. We will also present detailed modelling of all aspects of the observed polarimetry rather than just a simple consideration of the presence or absence of scattered broadened Hα emission in that paper.

2 THE SAMPLE AND OBSERVING DETAILS

2.1 Selection Method

Any test of AGN unification must use a sample selected on a known isotropic property since the unified model implies an orientation dependence for the type of Seyfert seen. It is important to avoid the error, often seen in the literature, that all Seyfert 2's are identical. If the unified model is correct, Seyfert 2s must have a wide range of orientation of the AGN axis with respect to our line of sight, from narrowly mis-aligned so that the Seyfert 1 core is only just out of view, to those where the broad and narrow line regions are almost entirely in the plane of the sky. It is highly unlikely that the observed properties of Seyfert 2's seen at widely different orientation angles are the same. Therefore it is not sufficient to pick a sample of Seyfert 2 galaxies at random from the literature, as any such sample will almost certainly be biased with respect to orientation.

In practice, a combination of extinction, opacity effects, and varying beam-size at different wavelengths, makes it impractical to select on any property related solely to the active nucleus. It is possible though to select based on intrinsic properties of the galaxy as a whole, in a wavelength regime where the active nucleus itself is likely to be important. Examples of this type include far infrared (hereafter FIR), cm radio, and global optical emission. Each of these has its own particular advantages and disadvantages, but we initially chose a FIR selection since there is a complete FIR selected galaxy database readily available.

The nature of the FIR emission in Seyfert galaxies was the subject of considerable speculation until relatively recently. The turnover in the spectral energy distribution beyond 100μm was seen as evidence for a thermal origin (Chini, Kreysa and Biermann 1989). More recent ISO photometry has helped to confirm that this picture is correct for most if not all nearby radio quiet AGN (eg Perez Garcia and Rodriguez Espinosa 2000). There have been many attempts to model the properties of the dust emission around the active nucleus itself in the context of the unified model (eg Pier and Krolik 1992, Laor and Draine 1993, Granato and Danese 1994, Efstathiou and Rowan-Robinson 1995). These models suggest that the 60–100μm emission from any AGN is largely unaffected by orientation.

Some fraction of the emission at these longer wavelengths could be due to the host galaxy rather than the core however. Star formation in particular gives rise to significant

FIR emission. It is possible however to distinguish the main source of the FIR emission using simple colour-colour diagrams of the observed IRAS fluxes (eg. Dopita et al 1998). Figure 1 shows IRAS colour-colour plots for the sample of galaxies considered by Kewley et al. (2000). That sample shares similar FIR selection criteria to those used in Paper 1 and this paper, but included all types of galaxy. The data shown here differ from that in Kewley et al. since we have revised the IRAS fluxes to use the data from the IRAS Bright Galaxy Survey (BGS: Soifer et al. 1989 and Sanders et al. 1995). The solid line in the figures represents the track for an increasingly reddened Seyfert galaxy, whereas the dashed line shows the locus of known starburst galaxies (see Dopita et al. 1998). Galaxies of mixed excitation should lie between these lines (the dot-dashed line shows the extreme mixing line between starburst and AGN activity). Seyfert galaxies of both types are shown in the left hand panel, and starbursts and LINERs in the right, in order to show the clear differences in their observed properties.

2.2 The Infrared Catalogue

We used the catalogue of IRAS galaxies and the redshift survey of Strauss et al. (1990, 1992) to identify our AGN sample. We did not rely on the Rush et al. (1993) catalogue used in Paper 1 for several reasons. First, it suffers badly from classification errors. This meant we had to independently classify all galaxies that met our selection criteria regardless of which source we used for the IRAS data. Secondly, the Strauss et al. catalogue is larger, and complete to fainter flux limits, making it better for identifying a larger parent sample of AGN. Lastly, doubts have been raised about the accuracy of the IRAS fluxes in the Rush et al. catalogue (Alexander & Aussel 2000).

Strauss et al. (1992) carried out a spectroscopic survey of sources selected from the IRAS Point Source Catalogue (PSC v2.0) by Strauss et al. (1990), to determine redshifts of the galaxies, and remove non-extragalactic sources. The actual IRAS fluxes they quote are not drawn solely from the PSC however. Where the PSC flags a source as extended or variable, Strauss et al. (1990) derived ADDSCAN fluxes. These should in principle be better than the PSC fluxes since (i) they correctly sum all the flux from an extended object and (ii) they coadd more of the raw IRAS data and are therefore of higher signal-to-noise. Strauss et al. (1990) discuss this issue at greater length. The final catalogue of Strauss et al. (1992) contains most galaxies in the original PSC down to a 60μm flux limit of 1.9Jy.

The IRAS fluxes actually quoted in this paper however are derived from a variety of sources, since we sought the best possible data once the initial selection was carried out. We compared the fluxes in Strauss et al., the IRAS Faint Source Catalogue Version 2 (FSC: Moshir et al. 1991), and the BGS (Soifer et al. 1989, Sanders et al. 1995). These all agree within the quoted errors for point sources. The BGS data are also ADDSCAN fluxes of the original raw data, but with a higher degree of rejection of 'bad' scans. They should therefore be more accurate than the Strauss et al. data. Therefore, for galaxies with $F_{60\mu m} > 5$Jy we used the fluxes from the BGS. We used the data of Strauss et al. (1990) for galaxies with $F_{60\mu m} < 5$Jy where those data were derived from ADDSCAN fluxes. Finally, for all other galaxies we used the data quoted in the FSC (which again is produced from coadding more of the raw IRAS data than the PSC). The BGS data quote errors on their fluxes, as does the FSC. We assume the errors on the Strauss et al. ADDSCAN fluxes must be bound by the FSC errors.

Our initial sample is based on those galaxies with good detections in the PSC (ie quality flag set to 3) at 60μm. They also have moderate or good detections at 25 and 100μm (quality flag set to either 2 or 3). We did not set any restriction on the 12μm data. However, because we do not use the actual PSC data in our analysis, all objects in our final sample actually have firm detections at all four IRAS wavebands.

2.3 Detailed Selection Parameters

The detailed selection criteria of our sample are as follows (some of these are actually imposed by using the Strauss et al. catalogue): $L_{FIR} > 10^{10}\,L_\odot$(where F_{FIR} has its usual definition – $F_{FIR} = 1.26\,(2.58F_{60\mu m} + F_{100\mu m}) \times 10^{-14}Wm^{-2}$); $F_{60\mu m}/F_{25\mu m} < 8.5$ which matches most known Seyferts (de Grijp et al. 1992) without requiring us to classify the large population of normal galaxies with cooler IRAS colours; $F_{60\mu m} > 3$Jy; Galactic latitude $|b| > 25°$; declination less than $+70°$; and classification as a Seyfert 2 (from our own spectroscopy if possible: see Section 2.5). We note that we class Seyfert 1.8 and 1.9 galaxies as Seyfert 2's for the purpose of this paper. We use a value of $H_0 = 75 kms^{-1}Mpc^{-1}$ throughout.

These criteria are looser than those adopted in Paper 1. Despite this, some of the galaxies discussed there do not fall into the current sample. These are NGC34 (more accurately classified as a LINER), NGC7496 and NGC7590 (both $L_{FIR} < 10^{10}\,L_\odot$). None of these objects showed evidence for an HBLR.

Table 1 lists the final sample of 28 galaxies that satisfy all our criteria. We do not have spectropolarimetry for 4 of these objects. All have cool colours, with $F_{60\mu m}/F_{25\mu m} > 6$. A detailed discussion of these sources is deferred until the Appendix, though we will note, where appropriate, the effect they have on our analysis.

2.4 Observations

Full details of the observing procedures and data reduction will be given in a future paper. With the exception of those objects for which we have used data available in the literature, all spectropolarimetry was obtained at either the AAT or WHT, on the nights of 16, 17 and 18 August 1995 (AAT), 29 July 1996 (WHT), 26, 27 and 28 August 1997 (AAT) and 7, 8, 9 and 10 March 1998 (WHT). Only the data from 1998 were obtained with the slit at the parallactic angle (mainly for reasons of practical convenience when carrying out spectropolarimetry). We centred the slit on the brightest part of the galaxy at approximately the V band. The conditions were photometric for the all except the night of 18 August 1995. Total exposure times were approximately two hours for all sources observed at the AAT, and one hour for the sources observed with the more efficient ISIS spectrograph at the WHT. Ideally, the observations would seek to achieve

a level consistent with that expected of any broad line in the scattered light (cf Section 3.1). In practice, instrumental and other effects limited us to a fixed small error in the polarization of $\sim 0.3\%$. The fainter sources, and some that were observed in adverse weather conditions, have larger observed errors. Fuller details of the errors will be given in the paper presenting the full data.

For the AAT data, we used the RGO Spectrograph together with a Tektronix 1024^2 CCD. For the WHT data, we used the red arm of the double beam spectrograph ISIS with a Tektronix 1024^2 CCD. A calcite prism was used in both instruments to split the incoming beam into *e* and *o*-rays together with an aperture mask made up of discrete slit-lets. A half-waveplate modulated the incoming phase. Four steps of the waveplate at 0°, 45°, 22.5° and 67.5° were required to derive the full set of Stokes parameters for linearly polarized light. The slit width was typically 2 arcseconds at the AAT, and 1–1.5 arcseconds at the WHT. We extracted data from a region of between 3 and 4 arcseconds along the slit in most cases. Sky subtraction was achieved by nodding the object into an adjacent slit-let. The data were reduced in a standard fashion. The effective spectral resolution is between 7 and 9Å for all data depending on the exact slit width used. The sky and object spectra for the four separate waveplate positions were extracted then combined to give the final Q, U and I Stokes parameters.

2.5 Spectral Classification

We measured the relative line fluxes from our spectra by fitting Gaussian profiles. Where the actual observed profile is highly non-Gaussian, we used a multiple component Gaussian fit to measure the total flux, since we are not interested in the detailed line profile information itself. We also allowed for the possibility of stellar Hβ absorption in our spectra. It is possible to overestimate the internal extinction, and misclassify starburst galaxies as AGN without this correction. We felt it was better to actually fit the absorption component directly rather than making an average correction as has often been done in the past. This will make little difference for galaxies with an old underlying stellar population, where the Hβ absorption is weak in any event, but has a significant effect on those galaxies which have a stellar continuum similar to that of an A star (essentially those galaxies with a post-starburst population).

The extinction was derived using the Whitford reddening curve as parameterized by Miller & Mathews (1972), assuming the intrinsic Hα/Hβ ratio is 3.1. The extinction corrected line ratios for our own spectra, and for those galaxies taken from the literature, are given in Table 2. We note that the derived $E(B-V)$ values may not be completely accurate since we did not observe at the parallactic angle for most of our observations. This is especially a problem for strongly nucleated sources observed well away from the parallactic angle, since a point source at the wavelength of Hβ will appear to shift by up to 1 arcsecond from its position at Hα due to differential atmospheric dispersion. Similarly, such effects can lead to errors in line fluxes that have been corrected for extinction. By contrast, line ratios, as long as they arise from the same component, are largely unaffected, since the extinction correction essentially forces the data to have the 'correct' spectral form. The same arguments can also be made regarding data taken under non-photometric conditions. These caveats also apply to much of the data presented in the literature, and should be borne in mind as a possible source of error in the extinction corrected [OIII] 5007Å line luminosities quoted in Table 2 and used throughout this paper.

We classified each galaxy based on the diagnostic diagrams of Veilleux and Osterbrock (1987). We also considered whether the galaxy showed evidence of HeII 4686Å emission. The high signal to noise of our spectropolarimetry data means we are able to detect this line where it is present. This line is, by definition, not seen in LINER galaxies. It is seen in some starburst galaxies, where it arises in the winds of Wolf-Rayet stars (see, eg, Vacca and Conti 1992). However, the feature in Wolf-Rayet galaxies is much broader than the other observed lines, whereas in all the galaxies we observed the width of the 4686Å line is consistent with the width of [OIII] 5007Å, indicating it also arises in the NLR.

Four of the galaxies included in Table 2 do not have standard Veilleux & Osterbrock Seyfert classification. We have kept these galaxies in our sample on the basis of other reported characteristics. 0031–2142 is classed as a Seyfert 1.8 by Moran et al. (1996) on the basis of weak broad Hα emission. Mrk 334 is classed as a Seyfert on the basis of a weak [FeX] line, which cannot arise in a LINER. 0019–7926 shows weak HeII emission. It also seems possible that we have not observed the actual nucleus. Both de Grijp et al. (1992) and Vader et al. (1993) present spectra of this galaxy which have a standard Seyfert classification on the basis of all the Veilleux & Osterbrock (1987) indices, as well as significantly stronger [OIII] 5007Å emission than is present in our spectrum. However, Kewley et al. (2001) present data that are in agreement with ours. Given the uncertainty we have decided to include this object. NGC 7582 shows weak HeII emission, and has been observed to show transient broad Hα (Arextaga et al. 1999). We tested for any effect that the inclusion of these galaxies had on the statistical tests that we describe in Section 3. There was no significant difference in any case. The only difference that their exclusion makes is to the overall detection rate reported in Section 3.1, and we discuss that factor there. We also discuss, where appropriate, any other effect that the inclusion of these galaxies may have.

3 RESULTS

3.1 The Polarimetry Data

Only one of the galaxies newly reported in this paper, NGC5995, contains an obvious HBLR. Broad Hα and Hβ are clearly evident in the polarized flux from this object (see Figure 2). Here we have plotted the Stokes flux from our observations (derived from the rotated Stokes parameter – these quantities are a less biased estimate of the actual polarization and polarized flux present since they are not positive biased – see Miller, Robinson and Goodrich 1988). The measured full width at half maximum of the broad Hα component is approximately 2700kms^{-1}. Although the data has lower signal-to-noise near Hβ we can also measure the Hα/Hβ ratio in our polarized flux spectrum. We obtain a

ratio of 18±6, which corresponds to $E(B-V) = 1.7 \pm 0.4$ assuming an intrinsic ratio of 3.1. We can compare this with the extinction value given in Table 2, which shows $E(B-V) = 1.78$. Given the similarity of these values it would appear that most of the extinction lies between us and the scattering particles or narrow line region, rather than between the AGN core and the scatterers. Finally, one other notable feature of the spectrum of NGC5995 is that it shows clear evidence for strong stellar absorption lines. This is rather unusual for HBLRs as noted by Kay and Moran (1998).

Two other galaxies show weak features that may be the signature of an HBLR. NGC5135 has a weak broad feature in the polarized flux, but no signature in the polarization itself. In addition, the residual broad feature left after subtracting out the narrow line component is considerably redshifted with respect to the systemic velocity (by more than 1000kms^{-1}). This could be due to the weakness of the feature however, since it is possible that we have over-corrected for the narrow Hα and [NII] components in the polarized flux spectra, and hence removed the blue 'wing' of the broad feature. NGC5929 shows a weak broad feature in the polarization at Hα but no evidence for a broad component in the actual polarized flux. Again, it is possible that a weak broad line could be masked by the much stronger polarized narrow lines. We do not therefore consider these features as detections of HBLRs in either galaxy, but clearly both sources are worthy of further study to confirm whether this is true.

We also considered whether we would expect to see an HBLR given the signal-to-noise achieved in these observations. We derived predicted broad Hα fluxes from the observed [OIII] 5007Å fluxes, with due correction for the difference in extinction between the two lines, but assuming that both the [OIII] emission from the NLR and the scattered light from the BLR suffer the same extinction along our line of sight. We used two methods for deriving the predicted flux. We fitted the observed relation between [OIII] 5007Å and broad Hα for the Seyfert 1s observed by Stirpe (1990), and then assumed that an average of 2% of the BLR light is scattered into our direction in Seyfert 2s (see Lumsden & Alexander in preparation) for the first prediction. For the second we fitted the observed relation between the scattered broad Hα flux and the direct [OIII] 5007Å flux in the HBLRs studied by Tran (1995a), Young et al. (1996a) and ourselves. The two results agree to within a factor of 5. We then derived an upper limit to the observed scattered broad Hα in our data from the Stokes flux, assuming the full width at half maximum of the line was 3600kms^{-1} (the average for the Seyfert 1s in Stirpe 1990). Where our limit is 3 times less than the predicted value in both cases we assume that the non-detection is secure. Where this condition is satisfied by only one of the predicted fluxes, we consider the non-detection is likely but flag the possibility that this is wrong in Table 2. In two cases, NGC7479 and 1408+1347, our limit is above the predicted values, and we cannot therefore rule out the presence of an HBLR. These results are broadly in line with the analysis of Alexander (2001) of the sample in Paper 1. Further observations of all the galaxies for which we cannot absolutely rule out the presence of an HBLR are clearly desirable. For the rest of this paper, however, we will assume that all of the galaxies in which we did not detect an HBLR are in fact non-HBLRs.

In total 8 out of the sample of 24 observed galaxies show evidence for a HBLR. Assuming the 4 unobserved galaxies with cooler IRAS colours are not HBLRs, this gives an overall detection rate of 29%. If we exclude the 4 galaxies with predominantly intermediate or LINER types discussed in section 2.5, the detection rate would be 8 out of 21 observed, and a total sample of 24. This gives a rate of 33%. Both of these are close to the value reported by Moran et al. (2000) based on an initial volume limited optical selection of 35%. The similarity probably indicates our initial selection is largely unbiased and provides a fair representation of the full range of nearby Seyfert 2s.

3.2 Optical and Infrared Diagnostics

Figure 3 shows where the HBLRs in our sample fall as a function of IRAS colour. Our expanded survey indicates that the trends we reported in Paper 1 still hold. There is a clear correlation between the mid-far infrared flux ratio and the ability to detect an HBLR. Galaxies with warmer colours ($F_{60\mu m}/F_{25\mu m} \lesssim 4$) almost uniformly show evidence for an HBLR: the two exceptions are the optically faint galaxies 0019–7926 and 0425–0440. As noted in Section 2.5 we may not have observed the nucleus of 0019–7926. If we have indeed misclassified this particular galaxy the net effect on our results is small as discussed in more detail in the Appendix. 0425–0440 is one of the galaxies in which we cannot rule out the possibility of a misclassification due to insufficient signal-to-noise.

Figure 3 can also be compared directly with Figure 1. It is clear that there is a greater spread in the Seyfert sample under consideration here than in the Kewley et al. (2000) sample. This is largely due to the inclusion of the galaxies which do not have standard Seyfert classifications (see Section 2.5), the low luminosity Seyferts in NGC5194 (M51) and NGC7172, and the inclusion of the galaxies for which we do not have spectropolarimetry (for which we are generally reliant on only one literature source for classification). In most of these cases it is likely from the IRAS data alone that the active core is not the dominant source of luminosity, since they follow the same track as the starburst and LINER population in Figure 1. By contrast the HBLRs uniformly follow the reddened Seyfert 1 track. The other striking aspect of the HBLRs from Table 2 is that they are always classified as Seyferts on the three standard Veilleux & Osterbrock classification diagrams. The HBLRs and the starburst/LINER dominated galaxies represent the two extremes in our data. The rest of the non-HBLR population lies between the two, with some on the Seyfert 1 reddening track, and some on the starburst/LINER track.

We considered whether luminosity is a factor in the detection of the HBLRs. A Mann-Whitney U test shows that the distributions of L_{FIR} for the HBLRs and non-HBLRs are consistent at the 95% level. Therefore L_{FIR} is not a factor in determining the presence of a HBLR, in agreement with our findings in Paper 1. A different result is obtained if we look at the [OIII] 5007Å line luminosity, $L_{\lambda 5007}$. It is generally held that the luminosity in this line is a good measure of the luminosity of the active core (Mulchaey et al. 1994; Alonso-Herrero, Ward and Kotilainen 1997). Our data suggest marginal support for there being a difference between

the HBLRs and non-HBLRs at the 10% significance level, in the sense that the HBLRs are more luminous on average.

If we look at how the IRAS colours behave as a function of $L_{\lambda 5007}$, we find that all galaxies with $L_{\lambda 5007} > 10^8\,L_\odot$ lie near the Seyfert 1 reddening line in Figure 3, regardless of whether they are HBLRs. This last point is confirmed by the weak correlation between $L_{\lambda 5007}$ and IRAS colour at a 5% significance level shown in Figure 4(a): the more luminous sources have warmer colours. There is no such correlation between L_{FIR} and colour as shown by Figure 4(b).

Another way to demonstrate the dependence of the IRAS fluxes on the AGN luminosity is to consider what fraction of the mid infrared flux actually arises near the active core. We have used the small aperture 10μm data presented in Giuricin, Mardirossian and Mezzetti (1995) and Maiolino et al. (1995) to determine how 'compact' the IRAS 12μm emission is. This is done in the standard fashion by defining a compactness parameter, C, which is the ratio of the small aperture 10μm flux and the IRAS 12μm flux scaled by an appropriate colour correction (Devereux 1987). The results are given in Table 3. Values of C near 1 indicate that the IRAS emission arises from within the aperture of the 10μm beam. Although only half of our sources have small aperture 10μm data, the results are instructive. All of the galaxies with $L_{\lambda 5007} > 10^{8.5}\,L_\odot$ have C$>$ 0.65. Only NGC5135 has a value of $L_{\lambda 5007} < 10^{8.5}\,L_\odot$ and a value of C larger than 0.65. These results are consistent with our findings above, since they indicate that the galaxies with lower AGN luminosities are more likely to show significant host galaxy emission in the mid infrared, which must also be true in the FIR as well.

We also used the equivalent width of the [OIII] line, $W_{\lambda 5007}$, as a measure of the ratio of the luminosities in the active core and the host galaxy. Figure 5 shows that $W_{\lambda 5007}$ and $L_{\lambda 5007}$ are correlated as might be expected, but only at the 10% significance level, and there is a large scatter. Galaxies with high values of $W_{\lambda 5007}$ tend to be more luminous, and to be more clearly classified as Seyferts (Table 2). In this sense, $W_{\lambda 5007}$ is a good indicator of whether or not the AGN dominates the optical spectrum and the overall spectral energy distribution.

In Figure 6(a) we show the relation between $W_{\lambda 5007}$ and $F_{60\mu m}/F_{25\mu m}$. Those galaxies which have large equivalent widths also show HBLRs. Formally, the galaxies with and without HBLRs have distributions of $W_{\lambda 5007}$ that are different at the 99% confidence level. There are counter examples, since NGC5995 and 0518–2524 both have values of $W_{\lambda 5007}$ which are more typical of the bulk of our sample. Those galaxies with the largest $W_{\lambda 5007}$ also have the warmest colours. Again this is consistent with the picture outlined above with regard to AGN luminosity and mid–far infrared colour.

As noted by Tran et al. (1999) and Alexander (2001) there is a clear trend for Seyfert 2s with HBLRs to have both warm IRAS colours and evidence for high excitation through the [OIII] 5007Å to Hβ ratio. Again, this is true for most of our sample. Figure 6(b) shows the extinction corrected [OIII] 5007Å to Hβ ratio as a function of $F_{60\mu m}/F_{25\mu m}$. Clearly, most of the HBLRs tend to have higher apparent excitation than the sample as a whole, and the two subsets are indeed statistically different at the 99.9% confidence level. This is not due to a dependence of the excitation on AGN luminosity as there is no correlation between the [OIII] 5007Å to Hβ ratio and $L_{\lambda 5007}$, nor is there a tendency for the more luminous AGN to have larger HeII 4686Å to [OIII] 5007Å line ratios as might be expected if there was such a correlation. A large [OIII] 5007Å to Hβ ratio is not a necessary requirement for an HBLR however: NGC5995 has a ratio ~ 6, closer to that of the non-HBLRs with standard Seyfert classifications in Table 2 (cf NGC5135 and NGC7130). Nor is a large [OIII] 5007Å to Hβ ratio a clear sign of an HBLR, or of warm IRAS colours, since there are galaxies in our sample with cool colours and large [OIII] 5007Å to Hβ ratio and without an HBLR.

3.3 Radio and X-Ray Properties of the Sample

The two other wavelengths with greatest power for examining the properties of the active core are cm radio and hard (2–10keV) x-ray. Shorter wavelength radio emission, and lower energy x-ray emission, can be due to thermal emission from star formation if present. We therefore searched the literature for both integrated and core radio fluxes at 2.3GHz, as well as the x-ray fluxes in the 2–10 keV band, and the neutral hydrogen column densities inferred from these. The data we used in our study are summarised in Table 3. The presence of many upper limits in the following requires the use of the techniques of survival analysis in comparing samples. We have made use of the software package ASURV, version 1.1 (La Valley, Isobe & Feigelson 1992), which implements methods for univariate and bivariate problems, as outlined in Feigelson & Nelson (1985) and Isobe, Feigelson & Nelson (1986).

One caveat should be made with regard to the core radio fluxes. Most of these values were obtained using the Parkes Tidbinbilla Interferometer (PTI), which linked the 64m Parkes antenna with the 70m Tidbinbilla antenna over a 275 km baseline. Most were obtained in snapshot mode, so if there is asymmetric structure on the scales to which the PTI is sensitive (~ 0.1 arcseconds) the flux will be underestimated if the PTI beam is not aligned with that structure. A comparison of the galaxies observed by both Sadler et al. (1995) and Thean et al. (2000) at 8.4GHz VLA show this effect clearly, even for some systems which are only marginally resolved by the PTI. However, most of our sources are likely to have unresolved cores, rather than more complex radio jet structures, and the PTI observations cover most of our sample, unlike the available VLA observations. Thean et al. (2000) did report detections of some compact cores at 8.4GHz for sources that have only upper limits in the PTI observations. We have not included these since it is clear from work such as Sadler et al. (1995) that the spectral index of the core varies widely, whereas the general emission from the galaxy is reasonably well matched to an index near -0.75. Furthermore, the 8.4GHz emission can be dominated by star formation. We note here though that at 8.4GHz the core in 0518–2524 contributes more than 50% of the total flux, whereas the cores in NGC4388 and NGC5194 contribute less than 10%. For comparison the 2.3GHz limits on all 3 are less than 10%.

There is no significant difference in the inferred core or total radio power between the galaxies showing evidence for an HBLR and those that do not. However, there is a weak,

though not statistically significant, trend for the HBLRs to have slightly higher core radio power. Unfortunately the limited amount of data available on the core radio fluxes and the large number of upper limits make it difficult to say whether this is real. There is also weak evidence (significance only 15% however) for the galaxies containing HBLRs to have higher ratios of core radio flux to far infrared flux (Figure 7a), but not higher ratios of integrated radio flux to far infrared flux (Figure 7b). These plots are essentially measures of how important star formation is to the radio and far infrared emission (see Helou, Soifer & Rowan-Robinson 1985). Galaxies in which the ratio of the total radio to FIR flux is high are likely to be AGN dominated. Figure 7 tends to indicate that most, but not all, HBLRs lie in systems in which the AGN dominates.

We also examined how well the radio luminosities correlated with the optical and infrared data. $L_{\lambda 5007}$ correlates very well with both the core and total radio power at better than the 99% confidence level. By contrast, L_{FIR} correlates with the total radio power at the 99% confidence level, but with the core radio power at only the 95% confidence level. The FIR-radio correlation for all radio quiet galaxies is well known (eg de Jong et al. 1985). The fact that Seyferts show a larger scatter in this relationship when compared to starbursts is also well known (Norris, Allen & Roche 1988, Sopp & Alexander 1991). A discussion of the relative contribution of the AGN core to the total flux can be found in Roy et al. (1994, 1998) and Heisler et al. (1998), who note that the scatter seen in the FIR–radio correlation is largely due to those galaxies with powerful radio cores. Our results are consistent with these findings. In particular, the tight correlation between $L_{\lambda 5007}$ and the core radio power strengthens the case for $L_{\lambda 5007}$ being a good measure of the AGN luminosity, and the poorer correlation between L_{FIR} and the core radio power indicates that L_{FIR} is not solely a measure of the AGN luminosity.

The 2–10keV x-ray band is important since it allows a clean measure of the intrinsic AGN flux, and many nearby AGN have been observed spectroscopically in that band by ASCA. For most of the galaxies in our sample the active core will be completely obscured below 2keV. The x-ray data can be used to derive the neutral hydrogen column densities to the central source. For sources with $N_H < 10^{24}\mathrm{cm}^{-2}$, the values are derived from the observed photoelectric cut-off. Sources with $N_H > 10^{24}\mathrm{cm}^{-2}$, often described as Compton thick, are obscured at 10keV, but may show reflection dominated spectra. The 'observed' extinction in these sources is therefore low since none of the direct flux actually reaches us. The inferred high column density is determined from other properties, such as the ratio of the observed 2–10keV flux with extinction corrected [OIII] 5007Å flux, which increases as the column density decreases, and the 6.4keV Fe Kα line equivalent width, which increases as the scattered component becomes more dominant. In a few cases, Compton thick sources have been observed with the BeppoSAX satellite, which can detect emission in the 10-100keV band as well. This allows more stringent limits to be placed in these cases (eg. Matt et al. 2000). The actual values as taken from the literature are given in Table 3, along with the original references.

For two of the objects in Table 3 we have used our own reductions of archived ASCA data. We only used the GIS2 and GIS3 data, and combined and grouped these data so that after rebinning there were at least 20 counts in each bin. We fitted absorbed power-laws plus a Gaussian (to represent the FeKα line) to the data in the 2–10keV range, analogous to the procedure in Bassani et al. (1999). This is actually a good fit to the observed spectrum of NGC5995, which is relatively bright and well detected by ASCA. The equivalent width of the best fit line is 240^{+240}_{-160}eV, and the photon index, $\Gamma = 1.8^{+0.14}_{-0.11}$. The rather low obscuring column seen is therefore intrinsic, and not due to us only seeing the source through scattered radiation. The ASCA data for IC3639 are of relatively low signal-to-noise, and allowed only a crude estimate of the equivalent width, of 4200^{+8000}_{-4200}eV, if the photon index was fixed at 2, and the line centre fixed at 6.34keV. However, this is consistent with the object being Compton thick, as also found by Risaliti, Maiolino and Salvati (1999). We use their value of N_H, derived from BeppoSAX data, since they determine a larger lower limit.

In Figure 8(a) we plot $W_{\lambda 5007}$ against N_H. There is a clear separation between the HBLRs and the non-HBLRs, in the sense that only the galaxies with the largest value of $W_{\lambda 5007}$ at any given obscuration show HBLRs. Figure 8(b) shows how the sample falls in the $L_{\lambda 5007}$–N_H plane instead. Although it is less clear cut, it is generally true that the galaxies with the largest values of $L_{\lambda 5007}$ at any given N_H show HBLRs (1925–7245 is the obvious exception here). Risaliti et al. (2000) reported an upper limit for the flux from 0019–7926. We have compared this limit with other data by ratioing with the extinction corrected [OIII] flux. This provides a crude measure of the obscuring column (eg Bassani et al. 1999). From this we conclude that $N_H > 10^{23}\mathrm{cm}^{-2}$. We did not plot this result on Figure 8 given the uncertainties involved, but we note that this limit is consistent with the results from the other non-HBLRs (though see also the discussion in the Appendix).

At some level the relatively smooth delineation between HBLRs and non-HBLRS in Figure 8(a) compared to the rougher trends seen in Figure 8(b) implies it is not simply AGN luminosity, but how that luminosity dominates over the host galaxy that is important in the detection of HBLRs. It should be noted that the separation seen in Figure 8(a) holds true even though there are many lower limits. Essentially these data points can only move to the right, and not vertically. The separation between the HBLRs and non-HBLRs at high column density is approximately a horizontal line in this plot, so the HBLRs and non-HBLRs from our sample can never mix in this diagram. Of course many of the non-HBLRs have not been observed in the hard x-ray band. However, all bar three of these galaxies have observed $W_{\lambda 5007}$ <40Å, and therefore are consistent with the trends already shown in Figure 8(a) regardless of what their x-ray properties might be. The exceptions are Mrk 1361, NGC 5929 and NGC 7592 which have $W_{\lambda 5007}$ ∼60Å. Hard x-ray observations of these galaxies would be valuable in determining whether the trends seen hold for the entire sample, as would spectropolarimetry of NGC 7592.

Finally, we note there is no correlation between N_H and IRAS colour, in agreement with Alexander (2001). This confirms the overall suspicion that IRAS colour is not directly linked to obscuration.

4 DISCUSSION

4.1 Analysis

It is worth stressing what our spectropolarimetric data actually reveal before considering how we can explain these observations. Clearly, the HBLRs, by definition, show evidence of an obscured (hidden) BLR, consistent with the predictions of the unified model. By contrast, we *cannot* say that the non-HBLRs do *not* contain a BLR. All we can say is that for the most part we do not detect scattered broad Hα from such a region at the level we would predict (see Section 3.1). For most of the non-HBLRs the signal-to-noise in our data is sufficient that we can strongly rule our such emission at the predicted level. The conclusion must be that any scattered emission from the BLR, if it exists in these galaxies, appears at a considerably lower level than our prediction on the basis of the behaviour of the known HBLRs. For some of the non-HBLRs we also know the BLR does exist from hard x-ray observations. Although not relevant to the discussion of why we see an optical HBLR in some galaxies, this does provide additional confirmation that the unified model is correct at some level, and indicates that the non detection of a HBLR is not because there is no BLR to see. Clearly it would be useful to have x-ray spectra of the entire sample. This should now be possible, even for the very faint Compton thick sources, using Chandra and XMM-Netwon.

It may also be true that with sufficient signal-to-noise we would discover broad Hα in spectropolarimetry in all Seyfert 2s. Clearly, our data shows that for many of the non-HBLRs the scattered flux must be significantly below our predicted values. Therefore only data which can actually probe an order of magnitude deeper in the scattered flux is probably of use. It may be that instrumental limitations on the accuracy that can be achieved in the error in the polarisation will actually prevent such observations from being achieved even with larger telescopes. The discussion below allows the possibility that every galaxy contains an HBLR, since our basic assumption in analysing these data is that all Seyfert 2s do contain a BLR. If we can actually detect such emission in the future, the debate would then centre on whether there are correlations between the detected scattered broad Hα flux and factors such as AGN luminosity rather than simple detectability. For the moment, however, we are limited to seeking an explanation as to why some galaxies show obvious HBLRs and others show nothing.

There is a relatively simple explanation for all our data, even though our results may appear rather complex at first sight. First we note the clear message from Figure 3 is that HBLRs do appear like reddened Seyfert 1s. This is evidence that the AGN largely dominates L_{FIR} in these systems at least. The radio data tend to support this conclusion. By contrast the non-HBLRs that lie along the starburst/LINER track clearly cannot have dominant AGN cores. Therefore the clear split in colour between the bulk of the non-HBLRs and the HBLRs is due to the relative luminosities of the AGN and the host galaxy as first proposed by Alexander (2001). The division between the two groups in the [OIII] 5007Å to Hβ ratio seen in Figure 6(b) is largely due to the same cause. The galaxies with prominent starbursts will have enhanced Hβ relative to [OIII] leading to lower ratios on average in the non-HBLR population. Another plausible reason for lower [OIII] 5007Å to Hβ ratios in some of the higher luminosity non-HBLRs is stratification in the NLR. If the higher excitation lines arise nearer the nucleus, as is often observed for Seyferts, more obscured objects will naturally have lower [OIII] 5007Å to Hβ ratios, and lower $W_{\lambda 5007}$ as well. This mechanism may explain the behaviour of some of the Compton thick non-HBLRs for example. However, both the IRAS colours and the optical line ratios are essentially secondary indicators of the underlying reason as to why we do or do not see HBLRs.

The dominant reason we see an HBLR in any galaxy is revealed when we study the galaxies at all wavelengths at which the AGN dominates. The HBLRs are (i) more luminous [OIII] 5007Å sources, and in particular have more prominent Seyfert characteristics in the optical with large equivalent width line emission; (ii) have more of their mid infrared flux arising from the region around the AGN; (iii) on average have brighter radio cores; (iv) have less obscuration than non-HBLRs of similar luminosity. The first three of these points indicate that there are two factors present: first how intrinsically luminous the AGN is, and second whether this dominates the luminosity compared to the rest of the emission from the host galaxy. Figure 8(a) indicates the second of these factors is as important as the first. Point (iv) indicates that orientation is still important (at least if we assume the bulk of the obscuration arises in a torus). Clearly, for a galaxy that is tilted further from our line of sight, there will be greater extinction towards the NLR, and hence the observed scattered light component will be fainter. This is certainly consistent with the results for those non-HBLRs which have good signal-to-noise data, where, as noted above, the limit on any broad Hα present is well below the expected value from previously known HBLRs.

The most obvious explanation as to why the AGN luminosity and its contribution to the bolometric luminosity are so vital is that more luminous AGN cores support larger extended scattering regions. Clearly, an extended region is required in those HBLRs where the obscuring column to the BLR is $> 10^{25}\mathrm{cm}^{-2}$. This region of high obscuration must itself be compact (cf the discussion on NGC1068 in the Appendix and in Risaliti et al. 1999). Our data cannot constrain the size of the scattering region however, though imaging polarimetry can. Infrared imaging polarimetry of NGC1068 and the considerably less luminous Circinus Galaxy (Packham et al. 1997, Lumsden et al. 1999, Ruiz et al. 2000) clearly shows that the latter has a smaller scattering region. Other observable indicators also tend to favour such a correlation between the size of the scattering region and the AGN luminosity (see Section 4.2). If this is correct then we predict that the size of the scattering region in the less luminous, non-HBLR, Compton thin galaxies must be small.

The alternative possibility is that we are simply limited by signal-to-noise in our polarimetry as claimed by Alexander (2001), and perhaps indicated by our analysis in Section 3.1 for some of the non-HBLRs. We made an additional test to determine whether signal-to-noise is a major factor in HBLR detectability by examining the x-ray data, since the broad Hα flux should scale with the x-ray flux. We compared the x-ray fluxes in the Compton thin galaxies to test whether they showed a difference between the HBLR and non-HBLR systems. There is a clear distinction between the two groups in terms of luminosity, with the HBLRs being more lumi-

nous as they are at other wavebands, but none in terms of detected flux. This suggests again that luminosity is the key factor rather than simple signal-to-noise. It may be the case that those galaxies with a high current star formation rate also have more molecular gas near the nucleus, making it easier to hide the NLR. Further infrared imaging polarimetry, which has the benefit of penetrating the obscuration whilst minimising any contribution to the polarization from the host galaxy, may allow us to isolate the scattering sites even in the less luminous or more heavily obscured systems and determine if it is the size of the scattering region or simply low signal-to-noise that best explains our results.

Better spatial and spectral resolution would also be a benefit in future spectropolarimetric surveys. Improved spatial resolution will allow the scattering region to be isolated, reducing the diluting contribution from the host galaxy, as appears to be the case for Circinus. This could be particularly important for those cases where there is significant star formation. Young stars are a likely candidate for many galaxies showing evidence for the so called second featureless continuum (Tran 1995b, and see also the discussion in Gonzalez Delgado et al. 1998). These stars may also help mask any polarization signal, since they dilute the direct flux component from the AGN, resulting in a lower net polarization. Improved spectral resolution will make it easier to remove the contribution of polarized narrow lines, as shown graphically by Young et al. (1996a) for the case of 0518–2524.

The presence of star formation is not in itself an argument against orientation dependent obscuration in the cooler galaxies however. At least for AGN of equivalent luminosity, galaxies with significant star formation in which the core is obscured are more likely to be characterised as having starburst activity than those where there is little obscuration. This may actually be the case for at least some of our sample, particularly for galaxies with approximately equal inferred AGN luminosity such as NGC5135, NGC7130, NGC5995 and 0518–2524, all of which show purely Seyfert indicators in the optical spectra. We know there must be a scattering region of some kind in the Compton thick objects NGC5135 and NGC7130, since the hard x-ray continuum from these objects is *reflected* light from the Seyfert 1 core. Again, we should be able to test the extent, and the extinction to this scattering region using infrared imaging polarimetry.

4.2 Comparison with other work

A detailed discussion of other observations from the literature of some of the galaxies in our sample is presented in the Appendix.

Kay and Moran (1998) and Moran et al. (2000) recently reported several new HBLRs. Examination of the IRAS fluxes of these galaxies show that they too have warm colours (with the exception of NGC3081 for which no IRAS data exist). The same is true of all other previously known HBLRs. Only three of the galaxies studied by Moran et al. have been observed in the hard x-ray band, including NGC3081, which has $N_H = 6600^{+1800}_{-1600} \times 10^{20}\mathrm{cm}^{-2}$. Of the other two, NGC2273 has $N_H > 10^{25}\mathrm{cm}^{-2}$ and the coolest colour with $\mathrm{F}_{60\mu\mathrm{m}}/\mathrm{F}_{25\mu\mathrm{m}} = 4.4$, and NGC4507 has $N_H = 2920 \pm 230 \times 10^{20}\mathrm{cm}^{-2}$ and $\mathrm{F}_{60\mu\mathrm{m}}/\mathrm{F}_{25\mu\mathrm{m}} = 3.1$ (where we have taken the neutral hydrogen column densities from Risaliti, Maiolino and Salvati 1999). Although the equivalent widths of [OIII] 5007Å are rarely reported, it is clear from the published spectra in Moran et al. that these galaxies all have $\mathrm{W}_{\lambda 5007} \gtrsim 100$Å, consistent with the trends we find. The same is also true of the high polarization HBLRs considered by Awaki et al. (2000), and those HBLRs found by Young et al. (1996a). In fact the only exception to the trend shown in Figure 8(a) that we could find in the literature was for Circinus, which has $\mathrm{W}_{\lambda 5007} \sim 30$Å, but $N_H = 4.3 \times 10^{25}\mathrm{cm}^{-2}$ (Matt et al. 1999). It may be that the proximity of Circinus (so that we have higher quality data, with better spatial resolution) is the major factor in enabling us to see the HBLR.

The case for an extended scattering region in the highest luminosity sources is also made, in part, by Awaki et al. (2000). They show that almost all of the highly polarized HBLRs found by Miller and Goodrich (1990) and Tran, Miller and Kay (1992) are Compton thick, and hence that we see the x-ray emission as well as the optical through scattered light. This implies the scattering region must project outside the area of highest obscuration in all these sources. Their analysis indicates the x-ray emission can arise up to 30pc away from the actual core, considerably larger than the putative 1pc scale height of a torus. Indeed it is possible that these most luminous Seyfert 2s only appear as such because they are largely edge-on. There is certainly a dearth of objects in the top left hand area of Figure 8(a), and of all the objects considered by Awaki et al. only Was 49b lies in this region. Perhaps such objects are in fact classified as reddened Seyfert 1s, or 1.5s, instead of Seyfert 2s. Lastly, we note that the split in x-ray behaviour reported by Awaki et al. between the highly polarized HBLRs from the Miller and Goodrich and Tran, Miller and Kay studies and their sample of 'normal' Seyferts is in fact primarily a split between those systems which are Compton thick and show only reflected emission from the core, and those in which the core can be seen through the obscuring material. The objects they report as non-HBLRs actually contain several known HBLRs (including four in the sample reported here), and therefore their comparison of the cause of the HBLR/non-HBLR split should be viewed instead as the split between Compton thick and Compton thin sources. Therefore the case they make that HBLRs must all be edge on is only strictly applicable to the highly polarized sources.

5 CONCLUSIONS

We have completed a survey of the spectropolarimetric properties of a far infrared selected sample of Seyfert 2s. Our sample spans a wide range of AGN core luminosity, and appears representative of the local Seyfert 2 population. We conclude the following from our data:

- The key factors determining the visibility of an HBLR are (i) AGN luminosity, and how much the AGN dominates the bolometric luminosity of the host galaxy and (ii) the level of obscuration to the AGN. There is strong evidence that these are the only substantially important factors (cf Figure 8a).
- We find a similar fraction of HBLRs in our sample as in the optically selected sample of Moran et al. (2000) of

29%. It is likely that higher quality observations, or those at longer wavelengths may help to increase this fraction.

• There appears to be a split in the properties of our sample between galaxies which have a dominant host galaxy component and those which have a dominant AGN component as determined by their optical spectral properties. There is support for the conclusions of Alexander (2001) that at least the former group have overall properties that reflect the the host galaxy rather than the AGN. There is also support for the opposite point of view for the AGN dominated sources, that their overall properties are largely determined by the AGN luminosity and its obscuration along our line of sight.

• Our data are still consistent with the unified model, though perhaps not in its simplest incarnation. For the subset of data for which both spectropolarimetry and x-ray spectroscopy exist, all show either scattered broad Hα, transmitted Seyfert 1 x-ray spectra or scattered hard x-ray continua, consistent with a central Seyfert 1 core. However, our results do seem to contradict the impression that has grown recently that only obscuration is important in determining the observational characteristics of these moderate luminosity AGN (see, eg, Veron-Cetty and Veron 2000).

Acknowledgements

We thank both the anonymous referee and David Alexander for useful suggestions that improved the presentation of this paper. We acknowledge awards of telescope time on the AAT and WHT from ATAC and PATT respectively. SLL acknowledges support from PPARC through the award of an Advanced Research Fellowship. SLL also thanks the Access to Major Research Facilities Program, administered by the Australian Nuclear Science and Technology Organisation on behalf of the Australian Government, for travel support for the observations reported here. This research has made use of the NASA/IPAC Extragalactic Database (NED) which is operated by the Jet Propulsion Laboratory, California Institute of Technology, under contract with the National Aeronautics and Space Administration.

References

Alexander, D.M., 2001, MNRAS, 320, L15
Alexander, D.M., Aussel, H., 2000, preprint
Antonucci, R. 1993, ARA&A, 31, 473
Antonucci, R., Miller, J.S. 1985, ApJ, 297, 621
Arextaga, I, Joguet, B., Kunth, D., Melnick, J., Terlevich, R.J., 1999, ApJ, L123
Awaki, H., Ueno, S., Taniguchi, Y., Weaver, K.A., 2000, ApJ, 542, 175
Bassani, L., Dadina, M., Maiolino, R., Salvati, M., Risaliti, G., della Ceca, R., Matt, G., Zamorani, G., 1999, ApJS, 121, 473
Bicay, M.D., Kojoian, G., Seal, J., Dickinson, D.F., Malkan, M.A., 1995, ApJS, 98, 369
Bransford, M.A., Appleton, P.N., Heisler, C.A., Norris, R.P., Marston, A.P., 1998, ApJ, 497, 133
Capetti, A., Axon, D.J., Macchetto, F., Sparks, W.B., Boksenberg, A., 1995, ApJ, 446, 155
Capetti, A., Axon, D.J., Macchetto, F.D., 1997, ApJ, 487, 560
Chini, R., Kreysa, E., Biermann, P.L., 1989, A&A, 219, 87
Clavel, J. et al., 2000, A&A, 357, 839
Colina, L., Sparks, W.B., Macchetto, F., 1991, ApJ, 370, 102
Colina, L., Lipari, S., Macchetto, F., 1991, ApJ, 379, 113
Condon, J.J., Helou, G., Sanders, D.B., Soifer, B.T., 1990, ApJS, 73, 359
Condon, J.J., Anderson, E., Broderick, J.J., 1995, AJ, 109, 2318
Condon, J.J., Cotton, W.D., Greisen, E.W., Yin, Q.F., Perley, R.A., Taylor, G.B., Broderick, J.J., 1998, AJ, 115, 1693
Coziol, R., Demers, S., Pena, M., Torres-Peimbert, S., Fontaine, G., Wesemael, F., Lamontagne, R., 1993, AJ, 105, 35
Dahari, O., 1985, ApJS, 57, 643
de Grijp, M.H.K., Keel, W.C., Miley, G.K., Goudfrooij, P., Lub, J., 1992, A&AS, 96, 389
de Jong, T., Klein, U., Wielebinski, R., & Wunderlich, E., 1985, A&A, 147, L6
De Robertis, M.M., Hutchings, J.B., Pitts, R.E., 1988, AJ, 95, 1371
Devereux, N., 1987, ApJ, 323, 91
Dopita, M.A., Heisler, C.A., Lumsden, S.L., Bailey, J.A., 1998, ApJ, 498, 570
Efstathiou, A., Rowan-Robinson, M., 1995, MNRAS, 273, 649
Feigelson, E.D., Nelson, P.I., 1985, ApJ, 293, 192
Gallimore, J.F., Baum, S.A., O'Dea, C.P., 1997, Nature, 388, 852
Giuricin, G., Mardirossian, F., Mezzetti, M., Bertotti, G., 1990, ApJS, 72, 551
Giuricin, G., Mardirossian, F., Mezzetti, M., 1995, ApJ, 446, 550
González Delgado, R.M., Heckman, T., Leitherer, C., Meurer, G., Krolik, J., Wilson, A.S., Kinney, A., Koratkar, A., 1998, ApJ, 505, 174
González Delgado, R.M., Heckman, T., Leitherer, C., 2001, ApJ, 546, 845
Granato, G.L., Danese, L., 1994, MNRAS, 268, 235
Guainazzi, M., Matt, G., Antonelli, L.A., Fiore, F., Piro, L., Ueno, S., 1998, MNRAS, 298, 824
Guainazzi, M., Molendi, S., Vignati, P., Matt, G., Iwasawa, K., 2000, New Astronomy, 5, 235
Heisler, C.A., Lumsden, S.L., Bailey, J.A., 1997, Nature, 385, 700
Heisler, C.A., Norris, R.P., Jauncey, D.L., Reynolds, J.E., King, E.A., 1998, MNRAS, 300, 1111
Helou, G., Soifer, B.T., Rowan-Robinson, M., 1985, ApJ, 298, L7
Ho, L.C., Filippenko, A.V., Sargent, W.L.W., 1997, ApJS, 112, 315
Huchra, J.P., Burg, R., 1992, ApJ, 393, 90
Inglis, M.D., Brindle, C., Hough, J.H., Young, S., Axon, D.J., Bailey, J.A., Ward, M.J., 1993, MNRAS, 263, 895
Inglis, M.D., Young, S., Hough, J.H., Gledhill, T., Axon, D.J., Bailey, J.A., Ward, M.J., 1995, MNRAS, 275, 398
IRAS Point Source Catalog, Version 2. 1988, Joint IRAS Science Working Group, US GPO, Washington DC

Isasawa, K., Fabian, A.C, Brandt, C.S., Crawford, C.S., Almaini, O., 1997, MNRAS, 291, L17
Isobe, T., Feigelson, E.D., Nelson, P.I., 1986, ApJ, 306, 490
Kay, L.E., 1994, ApJ, 430, 196
Kay, L.E., Moran, E.C., 1998, PASP, 110, 1003
Keel, W.C., Kennicutt, R.C., Hummel, E., van der Hulst, J.M., 1985, AJ, 90, 708
Kewley, L.J., Heisler, C.A., Dopita, M.A., Sutherland, R., Norris, R.P., Reynolds, J., Lumsden, S.L., 2000, ApJ, 530, 704
Kewley, L.J., Heisler, C.A., Dopita, M.A., Lumsden, S., 2001, AJ, 132, 37
Kii, T., Nakagawa, T., Fujimoto, R., Ogasaka, T., Miyazaki, T., Kawabe, R., Terashima, Y., 1996, in X-Ray Imaging and Spectroscopy of Hot Cosmic Plasmas, ed. F. Makino & K. Mitsuda (Tokyo: Universal Academy Press), 161
Laor, A., Draine, B.T., 1993, ApJ, 402, 441
LaValley, M., Isobe, T., Feigelson, E.D., 1992, BAAS, 24, 839
Lonsdale, C.J., Lonsdale, C.J., Smith, H.E., 1992, ApJ, 391, 629
Lumsden, S.L., Moore, T.J.T., Smith, C., Fujiyoshi, T., Bland-Hawthorn, J., Ward, M.J., 1999, MNRAS, 303, 209
Maiolino, R., Ruiz, M., Rieke, G.H., Keller, L.D., 1995, ApJ, 446, 561
Malaguti, G. et al., 1998, A&A, 331, 519
Matt, G., et al., 1997, A&A, 325, L13
Matt, G., et al., 1999, A&A, 341, L39
Matt, G., Fabian, A.C., Guainazzi, M., Iwasawa, K., Bassani, L., Malaguti, G., 2000, MNRAS, 318, 173
Miller, J.S., Mathews, W.G., 1972, ApJ, 172, 593
Miller, J.S., Robinson, L.B., Goodrich, R.W., 1988, in Instrumentation for Ground Based Astronomy, p 157, ed. L.B. Robinson, Springer, New York
Miller, J.S., Goodrich, R.W., 1990, ApJ, 355, 456
Miller, J.S., Goodrich, R.W., Mathews, W.G., 1991, ApJ, 378, 47
Moran, E.C., Halpern, J.P., Helfand, D.J., 1996, ApJS, 106, 341
Moran, E.C., Barth, A.J., Kay, L.E., Filippenko, A.V., 2000, ApJ, 540, L73
Morganti, R., Tsvetanov, Z.I., Gallimore, J., Allen, M.G., 1999, A&AS, 137, 457
Moshir, M., et al., 1991, Explanatory Supplement to the IRAS Faint Source Survey, Version 2. JPL, Pasadena
Muxlow, T.W.B., Pedlar, A., Holloway, A.J., Gallimore, J.F., Antonucci, R.R.J., 1996, MNRAS, 278, 854
Norris, R.P., Allen, D.A., Roche, P.F., 1988, MNRAS, 234, 773
Osterbrock, D.E. 1993, ApJ, 404, 551
Osterbrock, D.E., Martel, A., 1993, ApJ, 414, 552
Packham, C., Young, S., Hough, J.H., Axon, D.J., Bailey, J.A., 1997, MNRAS, 288, 375
Pappa, A., Georgantopoulos, I., Stewart G.C., 2000, MNRAS, 314, 589
Pérez García, A. M., Rodríguez Espinosa, J.M., 2000, preprint
Pier, A., Krolik, J., 1992, ApJ, 401, 99
Risaliti, G., Maiolino, R., Salvati, M., 1999, ApJ, 522, 157
Roy, A.L., Norris, R.P., 1997, MNRAS, 289, 824
Roy, A.L., Norris, R.P., Kesteven, M.J., Troup, E.R., Reynolds, J.E., 1994, ApJ, 432, 496
Roy, A.L., Norris, R.P., Kesteven, M.J., Troup, E.R., Reynolds, J.E., 1998, MNRAS, 301, 1019
Ruiz, M., Alexander, D.M., Young, S., Hough, J., Lumsden, S.L., Heisler, C.A., 2000, MNRAS, 316, 49
Rush, B., Malkan, M.A., Spinoglio, L., 1993, ApJS, 89, 1
Rush, B., Malkan, M.A., Edelson, R.A., 1996, ApJ, 473, 130
Ruiz, M., Rieke, G.H., Schmidt, G.D., 1994, ApJ, 423, 608
Sadler, E.M., Slee, O.B., Reynolds, J.E., Roy, A.L., 1995, MNRAS, 276, 1373
Sanders, D.B., Egami, E., Lipari, S., Mirabel, I.F., Soifer, B.T., 1995, AJ, 110, 1993
Schachter, J.F., Fiore, F., Elvis, M., Mathur, S., Wilson, A.S., Morse, J.A., Awaki, H., Iwasawa, K., 1998, ApJ, 503, L123
Schinnerer, E., Eckart, A., Tacconi, L.J., 1999, ApJ, 524, L5
Shields, J.C., Filippenko, A.V., 1996, A&A, 311, 393
Soifer, B.T., Boehmer, L., Neugebauer, G., Sanders, D.B., 1989, AJ, 98, 766
Sopp, H.M., Alexander, P., 1991, MNRAS, 251, 14P
Sopp, H., Alexander, P., 1992, MNRAS, 259, 425
Stauffer, J.R., 1982, ApJ, 262, 66
Stirpe, G.M., 1990, A&AS, 85, 1049
Strauss, M.A., Huchra, J.P., Davis, M., Yahil, A., Fisher, K.B., Tonry, J., 1992, ApJS, 83, 29
Su, B.M., Muxlow, T.W.B., Pedlar, A., Holloway, A.J., Steffen, W., Kukula, M.J., Mutel, R.L., 1996, MNRAS, 279, 1111
Telesco, C.M., Becklin, E.E., Wynn-Williams, C.G., Harper, D.A., 1984, ApJ, 282, 427
Terashima, Y., Ptak, A., Fujimoto, R., Itoh, M., Kunieda, H., Makishima, K., Serlemitsos, P.J., 1998, ApJ, 496, 210
Thean, A., Pedlar, A., Kukula, M.J., Baum, S.A., O'Dea, C.P., 2000, MNRAS, 314, 573
Tran, H.D., 1995a, ApJ, 440, 565
Tran, H.D., 1995b, ApJ, 440, 597
Tran, H.D., Miller, J.S., Kay, L.E., 1992, ApJ, 397, 452
Tran, H.D., Brotherton, M.S., Stanford, S.A., van Breugel, W., Dey, A., Stern, D., Antonucci, R., 1999, ApJ, 516, 85
Turner, T.J., George, I.M., Nandra, K., Mushotzky, R.F., 1997a, ApJ, 488, 164
Turner, T.J., George, I.M., Nandra, K., Mushotzky, R.F., 1997b, ApJS, 113, 23
Turner, T.J., Perola, G.C., Fiore F., Matt G., George, I. M., Piro L., Bassani L., 2000, ApJ, 531, 245
Ueno, S., 1997, PhD thesis, Kyoto Univ.
Ulvestad, J.S., Wilson, A.S., 1989, ApJ, 343, 659
Vader, J.P., Frogel, J.A., Terndrup, D.M., Heisler, C.A., 1993, AJ, 106, 1743
Vacca, W.D., Conti, P.S., 1992, ApJ, 401, 543
Veilleux, S., Osterbrock, D.E., 1987, ApJS, 63, 295
Veilleux, S., Kim, D.-.C, Sanders, D.B., Mazzarella, J.M., Soifer, B.T., 1995, ApJS, 98, 171
Véron, P., Goncalves, A.C., Véron-Cetty, M.P., 1997, A&A, 319, 52
Véron-Cetty, M.P., Véron, P., 2000, A&AR, 10, 81
Xue, S., Otani, C., Mihara, T., Cappi, M., Matsuoka, M., 1998, PASJ, 50, 519

Young, S., 2000, MNRAS, 312, 567
Young, S., Hough, J.H., Axon, D.J., Bailey, J.A., Ward, M.J., 1995, MNRAS, 272, 513
Young, S., Hough, J.H., Efstathiou, A., Wills, B.J., Bailey, J.A., Ward, M.J., Axon, D.J., 1996a, MNRAS, 281, 1206
Young, S., Packham, C., Hough, J.H., Efstathiou, A., 1996b, MNRAS, 283, L1

Appendix: Comments on Individual Sources

Many of the galaxies discussed in this paper have been the subject of other detailed individual studies. It is worth highlighting some aspects of these studies since they illuminate the possible underlying physical conditions.

0019–7926: As noted in Section 2.5 both de Grijp et al. (1992) and Vader et al. (1993) present spectra of this object showing clearer Seyfert characteristics. From the data in Vader et al. we estimate that $W_{\lambda 5007} \sim 200$Å, and the intrinsic line luminosity is ~ 6 times larger than that reported here. This would move 0019–7926 in Figure 8 from the non-HBLR region into the HBLR one. We therefore suspect that new spectropolarimetric observations may detect an HBLR in this system. If true, this would increase the distinction between the HBLRs and non-HBLRs in terms of $L_{\lambda 5007}$, but not significantly change our other conclusions.

NGC1068: This is the best studied of all the HBLRs currently known. We now know that the likely orientation of the parsec scale torus in this galaxy is nearly edge on from direct radio imaging (Gallimore, Baum and O'Dea 1997). Unfortunately, the structure of the inner regions of NGC1068 is actually rather complex, since there is a small parsec scale radio structure aligned with the axis of this torus that is also visible in [OIII] images and imaging polarimetry from HST (Muxlow et al. 1996, Capetti et al. 1995, Capetti, Axon and Macchetto 1997), but the larger scale radio structure and visible ionisation cones are rotated through $\sim 30^\circ$ relative to these (Capetti, Axon and Macchetto 1997).

This complexity may however help to explain the variant requirements of the x-ray and the optical/infrared data. The BeppoSAX data reported by Guainazzi et al. (2000) show evidence for considerable variability in the hard x-ray emission from NGC1068. They use this to constrain the location of the scattering medium at ∼1pc from the nucleus. Since the Fe Kα line is fed by resonance scattering from a largely neutral medium, it further implies the obscuring torus is also ∼1pc from the nucleus. Indeed, as has previously been noted (Risaliti et al. 1999), unless the bulk of the obscuration lies at small radii, the implied mass of molecular gas would exceed the observed virial mass in NGC1068 and other nearby AGN. However, there is also clearly scattering on larger scales as detected both in the near infrared by Packham et al. (1997) and Lumsden et al. (1999), and in the ultraviolet regime by Capetti et al. (1995). Young et al. (1996b) found that a large scale torus ($\sim$ 200pc) is required to explain the infrared data, whilst still requiring the inner scattering radius to be $\sim$ 1pc to explain the optical spectropolarimetry (Young et al. 1995). The solution to this apparent dichotomy lies in the fact that there are clearly two levels of obscuring source in NGC1068. The mid infrared polarimetry of Lumsden et al. (1999) requires a compact optically thick ($A_V \sim 100$) region around the BLR, with a more diffuse larger scale molecular cloud with $A_V = 30$ hiding that region and the inner scattering cones. This latter region is also revealed in maps of the molecular gas near the nucleus (Schinnerer, Eckart, and Tacconi 1999). Clearly this also implies however that the reflected x-ray component should itself be partially absorbed. In the case of NGC1068, if our estimate of the visual extinction is correct, and the conversion to a column density is $\sim 1/10$ that of the Galactic ISM (which is typical of AGN), then the implied $N_H \sim 5 \times 10^{21}$cm^{-2}. This is sufficiently small to remain unnoticed in the existing data. NGC1068 should be taken as a cautionary example that local conditions can play a large role in the final global spectral properties of a galaxy.

Finally, we note that the circumnuclear starburst that lies at a radius of $\sim$ 1kpc from the nucleus may actually dominate the far infrared flux from NGC1068 (Telesco et al. 1984). This suggests that the warmth of the infrared colours is in fact due to the dominance of the AGN component at shorter wavelengths.

0518–2524: The higher resolution optical spectrum we used in determining the line ratios in Table 2 (which will be discussed in greater detail in a paper in preparation) also shows that 0518–2524 has a strong Balmer absorption line spectrum in the blue. This is probably also the reason why many previous papers fail to detect the Hβ emission present. There is therefore clear evidence for a recent starburst episode in 0518–2524. In addition, Clavel et al. (2000) show that there is relatively strong PAH emission in the mid infrared spectrum of this object, which is usually taken as an indication of the 10μm emission being due in significant part to star formation. It is a moot point as to whether the large far infrared luminosity is due to any star formation or the obvious AGN activity. The relatively low $W_{\lambda 5007}$ and failure to detect a compact core at longer radio wavelengths when a prominent core exists at shorter wavelengths may indicate the former however. It is also notable that this galaxy has the coolest mid-far infrared colours of any of the HBLRs presented here, even though the inferred extinction to the core from the x-ray data is small, which also suggests there may be a significant contribution to L_{FIR} from something other than the AGN.

NGC4388: This galaxy is almost edge-on, so any obscuration hiding the BLR may actually be due in part to the host galaxy rather than a nuclear torus. Weak broad Hα has been detected in direct light in off nuclear positions by Shields and Filippenko (1996). They find that this is best explained as evidence for an HBLR, even though the direct evidence from polarimetry is actually marginal (Young et al. 1996a). The combination of both observations however gives greater confidence in the classification of this galaxy as an HBLR.

IC3639: This galaxy has been studied in detail in the optical and ultraviolet by Gonzalez Delgado et al. (1998) and Gonzalez Delgado, Heckman and Leitherer (2001). They find evidence for a recent burst of star formation in the nucleus which contributes an equal amount to the AGN component to the overall bolometric luminosity. The starburst does not dominate the optical continuum however, since an older population contributes a larger fraction of the light.

NGC5135 and NGC7130: Detailed optical and ultraviolet studies of these galaxies were carried out by Gonzalez Del-

gado et al. (1998) and Gonzalez Delgado, Heckman and Leitherer (2001). They found evidence that the optical continuum was dominated by a young starburst. As with IC3639, the starburst has a similar bolometric luminosity to the AGN.

NGC7582: This galaxy showed brief evidence of broad Hα in direct flux (Aretxaga et al. 1999), probably due to a lowering of the obscuring column density, since there is also evidence for considerable hard x-ray variability in this galaxy (Schachter et al. 1998; Xue et al. 1998). Turner et al. (2000) summarise the evidence for a 'patchy' torus in this source, and the alternative possibility that the broad permitted line arose in a supernova as suggested by Aretxaga et al. Turner et al. find that the best fit to their 2-100 keV BeppoSAX data requires an obscuring column of $1.4 \times 10^{23}\mathrm{cm}^{-2}$ which completely covers the source, plus a Compton thick absorber with $N_H \sim 1.6 \times 10^{24}\mathrm{cm}^{-2}$ which only covers 60% of it. Because the Compton thick component does not cover the entire source, 'holes' in the thinner component could lead to unobscured sight lines towards the BLR. The optical classification (Table 2) is a reflection of fact that there is significant ongoing star formation in this galaxy.

The galaxies without spectropolarimetry: Four of the galaxies in our initial sample do not have spectropolarimetry. There is little available data for two of these (NGC5427 and NGC5899) but they would appear to be typical of the other galaxies which have cool IRAS colours in our sample. NGC7592 (also known as Mrk928) has been the subject of considerable study. It consists of an interacting pair: the eastern component is classed as a pure starburst (Lonsdale, Lonsdale & Smith 1992). The western component is classed as a possible AGN (see Table 2), though clearly has characteristics of a transition or composite object. Veron, Goncalves, & Veron-Cetty (1997) discuss this aspect of the galaxy in more detail. It seems unlikely that any of these three galaxies will show evidence for an HBLR. The final 'unobserved' galaxy is 0031–2142. This system is a known luminous x-ray source (see Moran, Halpern & Helfand 1996), but has the appearance of a starburst galaxy from its optical spectrum. Only the presence of weak broad Hα led to its classification as a Seyfert. The recent x-ray study of Georgantopoulos (2000) has confirmed its identification as a marginally obscured Seyfert. We have shown where this galaxy falls on our N_H–$\mathrm{W}_{\lambda 5007}$ diagnostic plot. On the basis of this evidence it is possible that despite its cool colours this galaxy may show scattered broad Hα. Although the optical and FIR emission is dominated by the starburst component, the obscuration is low. In this sense it might be thought of as analogous to a system such as NGC5995, but with added star formation present. Spectropolarimetry of this source is certainly desirable.

Name	RA (1950)	Dec (1950)	cz (km/s)	$F_{12\mu m}$ (Jy)	$F_{25\mu m}$ (Jy)	$F_{60\mu m}$ (Jy)	$F_{100\mu m}$ (Jy)	L_{FIR} ($\log(L_\odot)$)	Flag
Mrk334	00 00 35.1	+21 40 52	6824	0.26±0.039	1.05±0.095	4.35±0.305	4.32±0.346	10.70	
0019−7926	00 19 52.2	−79 26 46	21502	0.36±0.035	1.27±0.055	3.16±0.134	2.94±0.151	11.58	
0031−2142	00 31 43.1	−21 42 52	8133	0.22±0.029	0.56±0.045	3.85±0.193	8.42±0.505	10.93	*
NGC1068	02 40 07.2	−00 13 29	1178	36.10±0.064	84.25±0.191	181.95±0.103	235.87±0.218	10.83	
NGC1143	02 52 38.8	−00 23 07	8654	0.27±0.030	0.58±0.028	5.06±0.058	11.45±0.198	11.12	
0425−0440	04 25 56.9	−04 40 25	4592	0.16±0.022	1.43±0.058	4.13±0.162	3.30±0.192	10.32	
0518−2524	05 18 58.6	−25 24 39	12567	0.74±0.021	3.50±0.025	13.95±0.031	12.52±0.081	11.73	
NGC4388	12 23 14.4	+12 56 22	2455	1.06±0.031	3.42±0.068	10.05±0.033	17.40±0.177	10.26	
IC3639	12 38 10.2	−36 28 51	3059	0.64±0.034	2.55±0.044	7.53±0.042	11.54±0.204	10.31	
MCG-3-34-64	13 19 42.8	−16 27 55	4999	0.93±0.040	2.95±0.041	6.07±0.039	5.93±0.137	10.58	
NGC5135	13 22 56.7	−29 34 25	3923	0.62±0.038	2.53±0.053	17.10±0.060	29.50±0.179	10.90	
NGC5194	13 27 45.3	+47 27 24	579	11.00±0.100	15.00±0.150	98.80±0.988	280.40±2.804	10.10	
NGC5256	13 36 14.1	+48 31 52	8353	0.28±0.026	1.13±0.037	7.19±0.032	10.35±0.163	11.18	
Mrk1361	13 44 36.5	+11 21 15	6747	0.17±0.039	0.84±0.101	3.28±0.394	3.73±0.373	10.63	
NGC5427	14 00 48.3	−05 47 25	2647	1.14±0.043	1.33±0.070	9.93±0.056	24.81±0.120	10.40	*
1408+1347	14 08 16.6	+13 47 32	4837	0.13±0.023	1.04±0.073	3.69±0.258	2.87±0.201	10.31	
NGC5899	15 13 15.0	+42 14 06	2706	0.52±0.042	0.51±0.041	4.13±0.207	11.43±0.572	10.05	*
NGC5929	15 24 20.6	+41 50 57	2708	0.43±0.033	1.62±0.026	9.14±0.041	13.69±0.124	10.28	
NGC5995	15 45 37.4	−13 36 17	7297	0.53±0.041	1.40±0.098	3.95±0.277	6.70±0.536	10.82	
1925−7245	19 25 27.8	−72 45 39	18339	0.23±0.020	1.34±0.024	5.30±0.031	6.70±0.165	11.68	
IC5063	20 48 11.7	−57 15 26	3321	1.16±0.025	4.00±0.033	6.11±0.041	4.31±0.206	10.19	
NGC7130	21 45 19.7	−35 11 03	4875	0.62±0.020	2.18±0.029	16.91±0.045	25.97±0.161	11.06	
NGC7172	21 59 07.0	−32 06 42	2622	0.49±0.029	0.94±0.008	5.99±0.026	12.02±0.107	10.12	
NGC7479	23 02 26.6	+12 03 08	2586	1.40±0.037	3.92±0.066	15.35±0.060	24.60±0.308	10.49	
IC5298	23 13 31.2	+25 16 48	8449	0.32±0.033	1.88±0.061	8.75±0.052	11.64±0.123	11.23	
NGC7582	23 15 38.1	−42 38 40	1552	2.30±0.030	7.49±0.028	51.64±0.108	78.36±0.121	10.55	
NGC7592	23 15 47.5	−04 41 20	7480	0.27±0.034	0.95±0.067	8.02±0.053	10.50±0.149	11.09	*
NGC7674	23 25 24.7	+08 30 14	8895	0.68±0.043	1.88±0.044	5.28±0.048	7.91±0.171	11.08	

Table 1. Complete IRAS selected sample for spectropolarimetry observations. Redshift data are taken from Strauss et al. (1992). IRAS fluxes are derived from the IRAS BGS survey (Soifer et al. 1989; Sanders et al. 1995) except for 0019−7926, NGC5995 and NGC5899 which are from Strauss et al. (1990), and Mrk334, 0031−2142, 0425−0440, Mrk1361 and 1408+1347 which were taken from FSC. Galaxies which have a $*$ in the flag column do not have spectropolarimetry.

Name	HBLR?	Ref	E(B–V)	$\frac{[OIII]}{H\beta}$	$\frac{[OI]}{H\alpha}$	$\frac{[NII]}{H\alpha}$	$\frac{[SII]}{H\alpha}$	$\frac{HeII}{H\beta}$	$W_{\lambda 5007}$	$F_{\lambda 5007}$	Classification (1)	(2)	(3)	(4)	Ref
Mrk334	n?	b	0.69	0.23	−1.28	−0.23	−0.55	0.00	27.0	2.00	L	I	I	N	1 2
0019−7926	n	a	0.84	0.47	−1.36	−0.31	−0.51	−1.18	30.7	0.13	I	I	I	S	3
0031−2142			0.44	−0.03	−1.30	−0.35	−0.67		10.0	0.12	I	H	I		4 5
NGC1068	y	cd	1.02	1.07	−0.87	0.24	−0.53	−0.43	460.0	47.00	S	S	S	S	3 4
NGC1143	n	a	0.75	1.17	−0.70	0.33	−0.04	−0.76	34.7	0.48	S	S	S	S	3
0425−0440	n?	a	1.93	0.81	−0.69	−0.05	−0.41	< −0.36	6.6	1.30	S	S	S	N	3
0518−2524	y	e	0.32	1.05	−0.55	0.30	−0.23	−0.26	45.3	1.30	S	S	S	S	3
NGC4388	y	e	0.61	1.05	−0.80	−0.24	−0.21	−0.62	908.0	2.20	S	S	S	S	7 8
IC3639	y	a	0.85	0.91	−0.82	−0.09	−0.37	−0.78	110.0	3.40	S	S	S	S	3
MCG-3-34-64	y	e	0.30	1.06	−0.64	0.10	−0.38	−0.41	191.0	4.00	S	S	S	S	9
NGC5135	n	a	0.78	0.82	−1.25	−0.09	−0.54	−0.64	82.7	2.30	S	S	S	S	3
NGC5194	n?	a	0.97	1.05	−0.74	0.51	−0.03	< −0.51	11.0	2.20	S	S	S	N	3
NGC5256	n	a	0.51	0.67	−1.20	−0.24	−0.47	−0.69	101.1	0.21	S	S	S	S	3
Mrk1361	n	a	1.08	0.70	−1.10	−0.14	−0.72	−0.90	80.0	1.80	S	I	S	S	3
NGC5427			0.00	0.91	−0.57	0.21	−0.29		35.0	0.09	S	S	S		10
1408+1347	?	a	1.04	0.67	−0.77	0.11	−0.21	< −1.09	24.3	0.08	S	S	S	N	3
NGC5899			0.58	1.02	−0.64	0.32	−0.05		45.0	0.41	S	S	S		11
NGC5929	n	a	0.37	0.59	−0.67	−0.32	−0.24	−0.91	58.9	1.53	S	S	S	S	3
NGC5995	y	a	1.78	0.80	−1.23	0.01	−0.65	< −0.75	19.6	6.60	S	S	S	N	3
1925−7245	n	a	1.91	0.60	−0.64	−0.05	−0.62	< −1.44	56.5	2.20	S	I	S	N	3 12
IC5063	y	f	0.40	1.02	−1.59	−0.28	−0.40	−0.80	171.0	1.10	S	S	S	S	13
NGC7130	n	a	0.75	0.78	−1.06	−0.01	−0.54	−0.85	95.4	2.50	S	S	S	S	3
NGC7172	n?	a	0.89	0.68	−0.93	0.05	−0.29	< −0.69	7.6	0.07	S	S	S	N	3
NGC7479	?	a	1.11	0.62	−0.79	0.06	−0.14	< −0.17	7.0	1.00	S	S	S	N	3
IC5298	n?	a	0.90	0.60	−1.31	0.03	−0.65	−0.53	19.2	1.70	S	I	I	S	3
NGC7582	n	a	0.82	0.35	−1.66	−0.20	−0.60	−0.94	34.8	1.60	L	I	H	S	3
NGC7592			0.55	0.40	−1.18	−0.20	−0.43		60.0	0.39	I	L	S		14 15
NGC7674	y	eg	0.37	1.01	−0.58	0.01	−0.15	−1.10	584.0	1.70	S	S	S	S	1 16

Table 2. Optical properties of the sample. The second column indicates whether we detected a HBLR in our spectropolarimetric data. A n? indicates that no HBLR was detected, but that we cannot absolutely rule out the possibility that one exists with the current signal-to-noise of our data, as discussed in Section 3.1. A ? indicates the signal-to-noise is likely to be insufficient to determine whether an HBLR is present or not. A blank in this column indicates the object was not observed. The third column gives the reference for the optical spectropolarimetry. The codes are as follows: a – this work; b – Ruiz et al. (1994); c – Antonucci & Miller (1985); d – Inglis et al. (1995); e – Young et al. (1996); f – Inglis et al. (1993); g - Miller & Goodrich (1990). The other columns give the properties as derived from the direct fluxed spectra. The fourth column is the extinction, derived assuming the intrinsic Hα/Hβ ratio is 3.1. Columns 5–9 give the extinction corrected ratios (as $\log 10$(ratio)) for (5) $\frac{5007\mathring{A}\ [OIII]}{H\beta}$, (6) $\frac{6300\mathring{A}\ [OI]}{H\alpha}$, (7) $\frac{6584\mathring{A}\ [NII]}{H\alpha}$, (8) $\frac{6717+6731\mathring{A}\ [SII]}{H\alpha}$ and (9) $\frac{4686\mathring{A}\ HeII}{H\beta}$. Column 10 gives the equivalent width of the 5007Å [OIII] line in –Å, and column 11 the extinction corrected flux in the 5007Å [OIII] line in units of 10^{-12}erg s^{-1} cm^{-2}. Columns 12–15 give the derived classification following Veilleux & Osterbrock (1987) from (12) $\frac{[OIII]}{H\beta}$ versus $\frac{[NII]}{H\alpha}$; (13) $\frac{[OIII]}{H\beta}$ versus $\frac{[SII]}{H\alpha}$; (14) $\frac{[OIII]}{H\beta}$ versus $\frac{[OI]}{H\alpha}$; (15) presence of HeII emission. The codes are as follows: I – intermediate classification; L – LINER; N – no detection; S – Seyfert. Finally, the reference for the source of the spectral data is given (which in some cases is not the same as the source of the spectropolarimetric data). Where more than one letter is given, the first refers to the source of the line ratios, and the second to the source of the equivalent width of the [OIII] 5007Å line. The references are as follows: (1) Osterbrock & Martel (1993) – Seyfert classification is based on the probable detection of [FeX] by Osterbrock & Martel, which would not be expected in a typical LINER; (2) Dahari (1985); (3) this work or other unpublished data of our own; (4) Coziol et al. (1993); (5) Moran, Halpern & Helfand (1996) classify this as a Seyfert 1.8 on the basis of weak broad Hα; (6) Kewley et al. 2000; (7) Ho, Filippenko & Sargent (1997); (8) Young et al. (1996); (9) De Robertis, Hutchings & Pitt (1988); (10) Keel et al. (1985); (11) Stauffer (1982); (12) Colina, Lipari & Macchetto (1991); (13) Colina, Sparks & Macchetto (1991); (14) Lonsdale, Lonsdale & Smith (1992); (15) Kewley et al. (2001); (16) Veilleux et al. (1995).

Name	C	Core Flux	Total Flux	Refs	$F_{2-10\mathrm{keV}}$	N_H	Refs
Mrk334	0.95	< 5	18	a			
0019–7926		4	16	ba	<0.10		1
0031–2142					0.80	180^{+450}_{-170}	2
NGC1068	0.89	97	3290	ac†	3.50	$> 10^5$	3
NGC1143		4	99	bc			
0425–0440			29	d*			
0518–2524	1.00	< 3	25	ba	4.30	490^{+10}_{-16}	4
NGC4388	0.57	< 6	84	ac†	12.00	4200^{+600}_{-1000}	5
IC3639		14	59	ec†	0.13	$> 10^5$	6 7
MCG-3-34-64	0.67	26	176	a	2.10	7600^{+1300}_{-1220}	8
NGC5135	0.79	< 5	133	a	0.20	$> 10^4$	9
NGC5194			157	c†	1.10	$5 - 10 \times 10^3$	10
NGC5256	0.16		78	c	0.56	$> 10^5$	1
Mrk1361			38	f*			
NGC5427	0.04		20	gh†			
1408+1347		< 3	5	da			
NGC5929	0.08	1	73	ic†			
NGC5995			21	j*	22.00	86^{+40}_{-30}	7
1925–7245		33	180	bk*	0.38	$10^3 - 10^4$	11
IC5063		152	747	dl	13.10	2200^{+220}_{-200}	9
NGC7130	0.65	14	120	ec†	0.51	$> 10^4$	6
NGC7172	0.43	3	24	bc†	13.00	861^{+79}_{-33}	12
NGC7479			76	gm†			
IC5298			25	n*			
NGC7582	0.62	< 5	132	bo†	13.20	739^{+146}_{-100}	9
NGC7592	0.35		52	fg†			
NGC7674	0.85	38	133	ec†	0.50	$> 10^5$	13

Table 3. Data taken from the literature on the compactness of the 10μm emission, C, compact radio flux, integrated radio flux (both in mJy, and measured at 2.3GHz), observed hard x-ray flux (in units of 10^{-12}ergs s^{-1} cm^{-2} and measured in the 2–10keV band) and inferred neutral hydrogen column density (in units of 10^{20}cm^{-2}) from the x-ray data. Where an entry is left blank no data exists in the literature for that particular item for that galaxy. The 10μm compactness parameter, C, is either taken from Giuricin, Mardirossian & Mezzeti (1995), or derived from data presented in Maiolino et al. (1995), with the exception of NGC1068 where the flux used is taken from Lumsden et al. (1999). Radio data are taken from the following references: (a) Roy et al. (1998); (b) Roy et al. (1994); (c) Rush, Malkan & Edelson (1996); (d) Heisler et al. (1998); (e) Sadler et al. (1995); (f) Bicay et al. (1995); (g) Condon et al. (1990); (h) Morganti et al. (1999); (i) Su et al. (1996); (j) Condon et al. (1998); (k) Roy & Norris (1997); (l) Bransford et al. (1998); (m) Condon, Anderson & Broderick (1995); (n) Sopp & Alexander (1992); (o) Ulvestad & Wilson (1984). Where more than one reference is given, and a core flux is present, the core flux comes from the first listed, and the total flux from the second. If more than one reference is given, and there is no core flux, we have had to extrapolate the total flux from more than one source. Where the reference is marked with a *, the total flux has been extrapolated to 2.3GHz assuming a spectral index of –0.75. The total flux is interpolated from published data (usually at 1.5 and 5GHz) where the reference is marked with a †. The same is true for the core flux in the case of NGC5929. X-ray data are taken from: (1) Risaliti et al. (2000); (2) Georgantopoulos (2000); (3) Matt et al. (1997); (4) Kii et al. (1996); (5) Isasawa et al. (1997); (6) Risaliti et al. (1999); (7) this work; (8) Ueno (1997); (9) Turner et al. (1997b); (10) Terashima et al. (1998); (11) Pappa, Georgantopoulos and Stewart (2000); (12) Guainazzi et al. (1998); (13) Malaguti et al. (1998). We have made use of the catalogue presented by Bassani et al. (1999) in compiling these x-ray data.

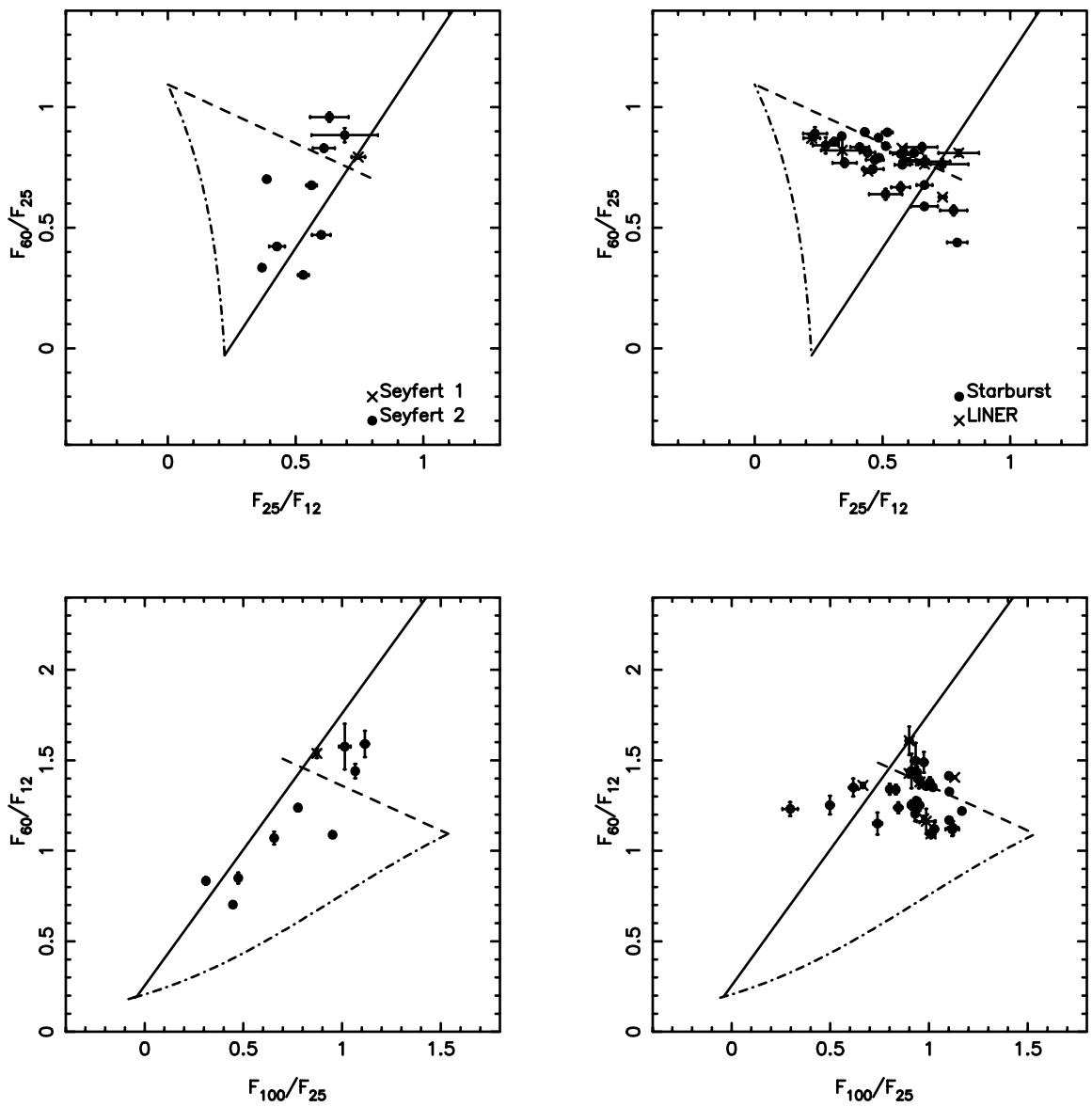

Figure 1: IRAS colour-colour plots of galaxies from the survey of Kewley et al. (2000). Seyfert 1 and 2s are shown in the left-hand panels, and starburst and LINERs (which have similar colours since LINERs tend to be dominated by the Galactic component as far as their IRAS colours are concerned) in the right-hand panels. The solid line is the reddening line for Seyfert galaxies derived by Dopita et al. (1998). The dashed line is the locus of starburst galaxies found by the same authors, and the dot-dashed line represents the maximal extent of the region occupied by galaxies of mixed excitation.

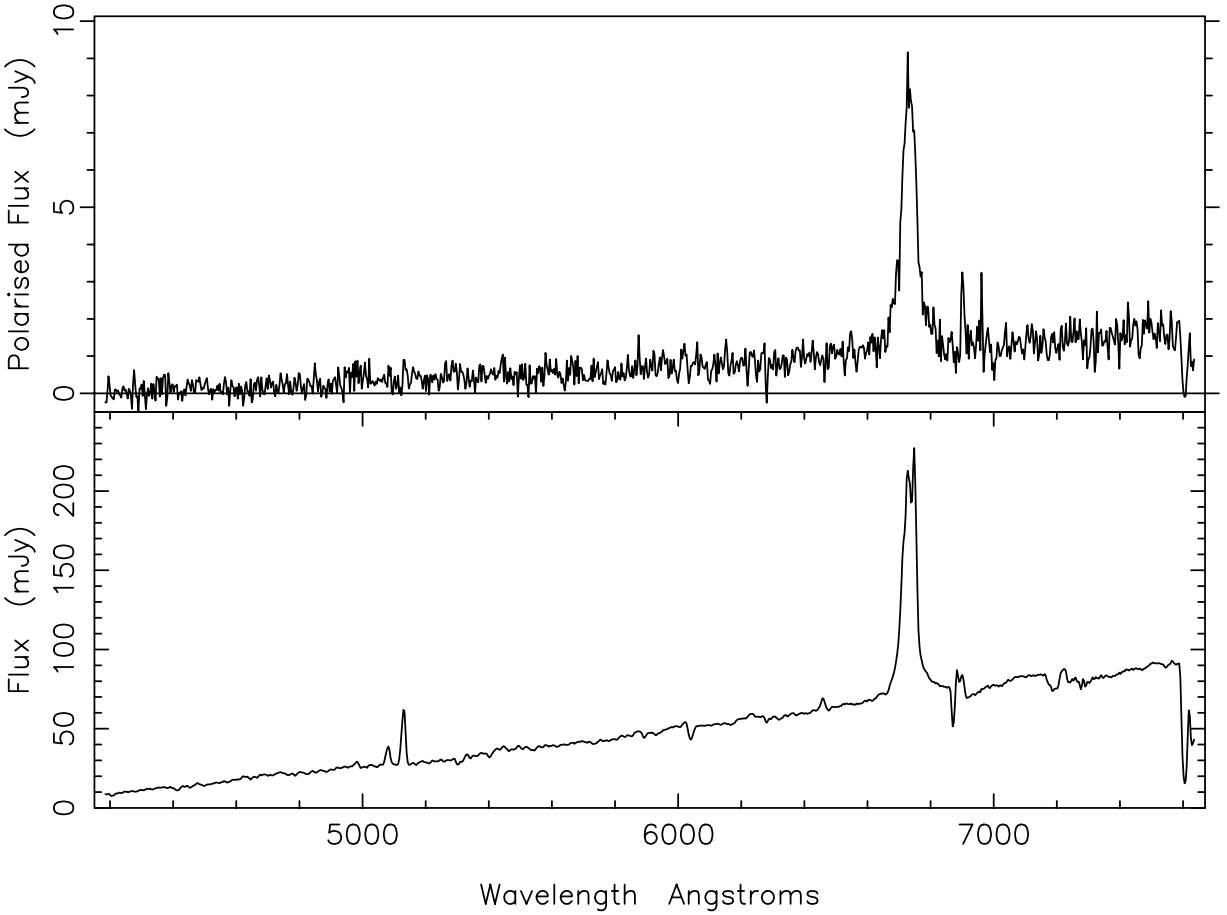

Figure 2: Spectropolarimetry of NGC5995. The broad Hα is clearly evident in the polarized flux. Weak broad Hα is also present in the direct spectrum, leading to a classification for this galaxy as a Seyfert 1.9.

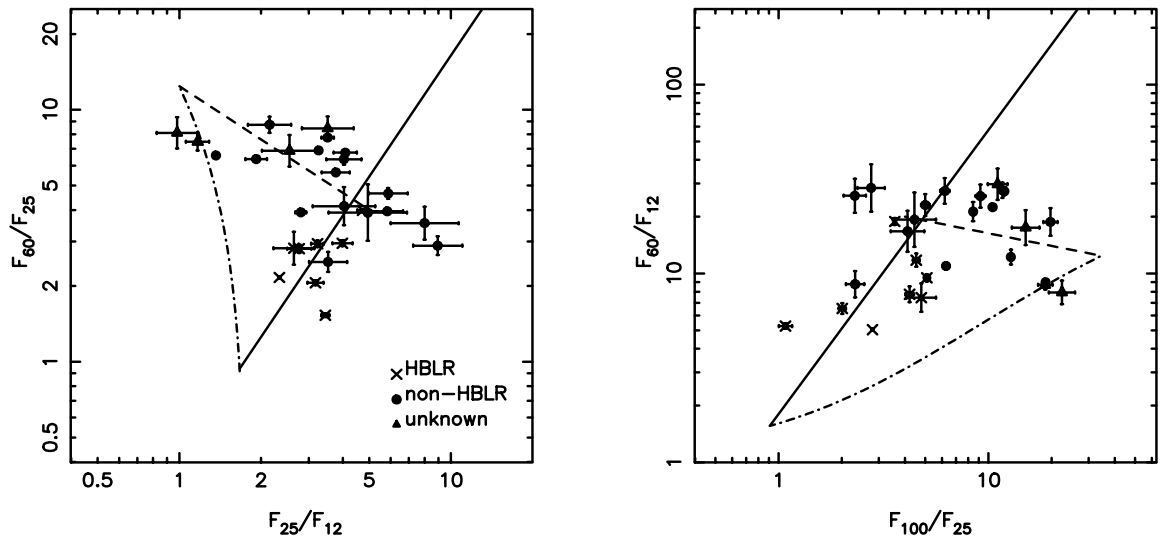

Figure 3: IRAS colour-colour plots as in Figure 1, but for the sample of Seyferts considered here. The crosses represent those galaxies in which an HBLR has been detected, the solid circles are those galaxies without a detection and the triangles are those galaxies for which we do not have spectropolarimetry. Note how the HBLRs tend to congregate on the Seyfert reddening line, in the region of warmer IRAS colours. Some of the Seyferts considered clearly do not have colours dominated by the AGN from this plot, since they have colours similar to the starburst/LINER population in Figure 1.

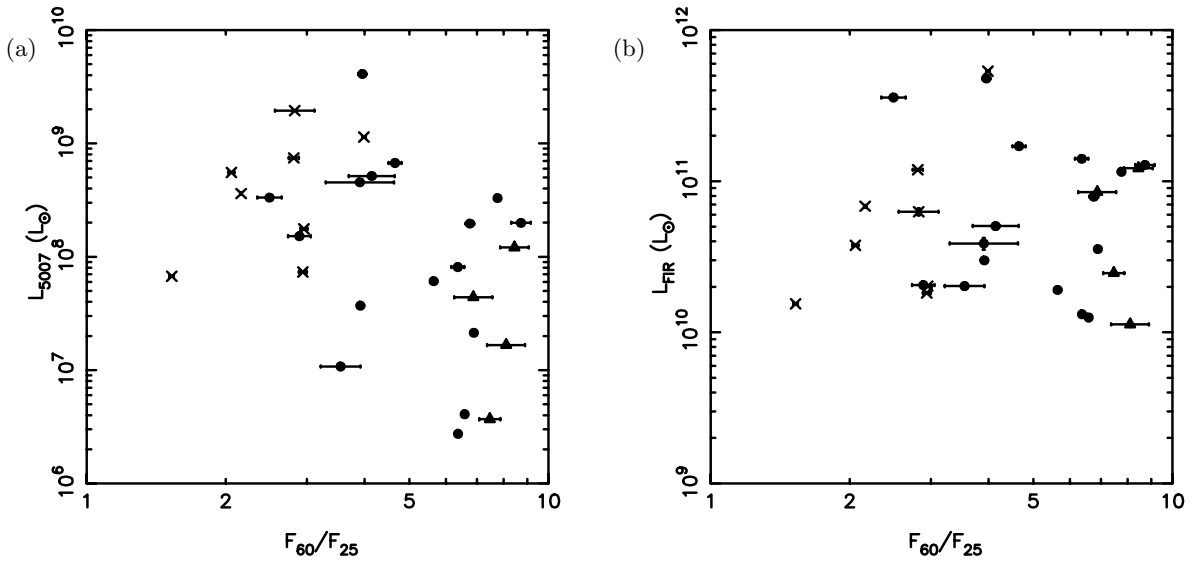

Figure 4: (a) $L_{\lambda 5007}$ and (b) L_{FIR} as a function of IRAS mid–far infrared colour. There is a weak correlation present in (a) but not in (b), suggesting that the $L_{\lambda 5007}$, but not L_{FIR}, is a factor in the observed colour. The symbols are as in Figure 3.

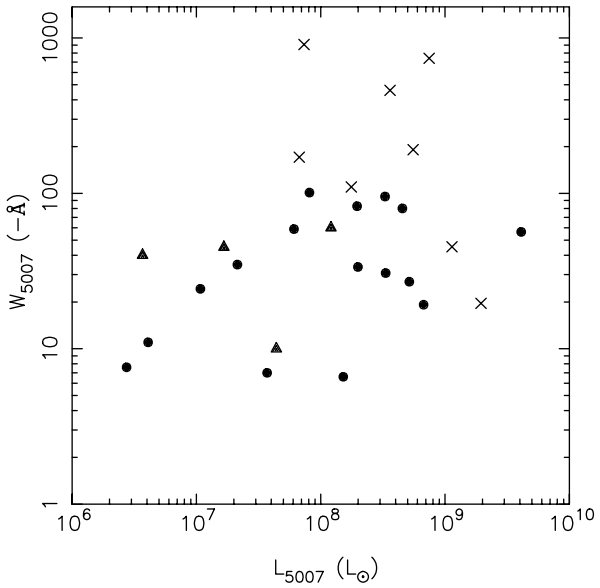

Figure 5: The correlation between the [OIII] 5007Å line equivalent width and the extinction corrected [OIII] 5007Å luminosity. The symbols are as in Figure 3.

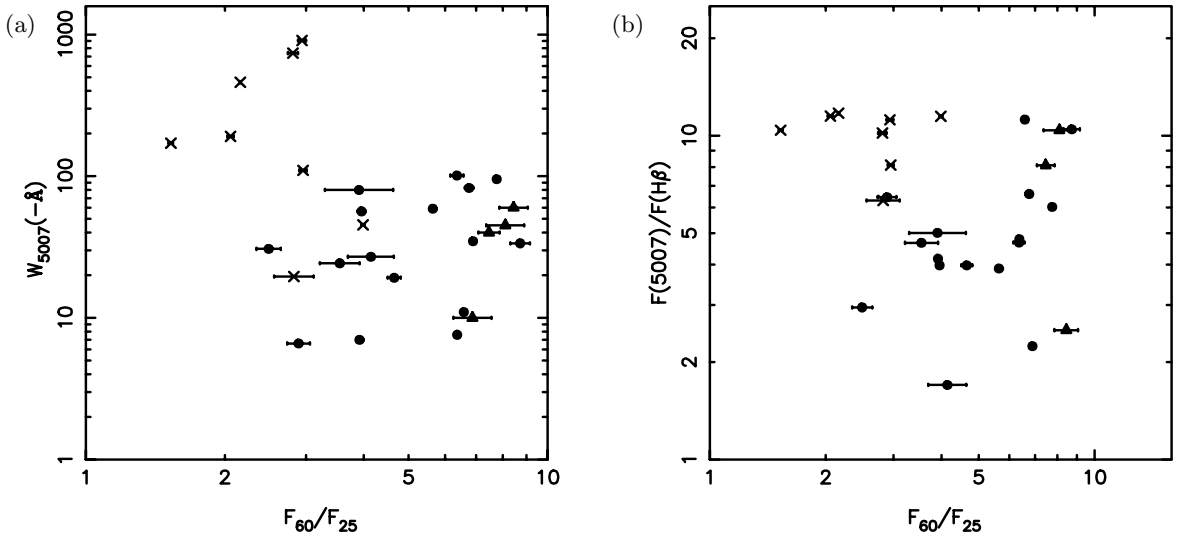

Figure 6: The observed correlation between (a) the equivalent width of [OIII] 5007Å, and (b) the extinction corrected [OIII] 5007Å to Hβ ratio, and the IRAS mid–far infrared colour. On average the HBLRs have larger absolute equivalent widths, and higher values of the optical line ratio. The symbols in (a) are as in Figure 3.

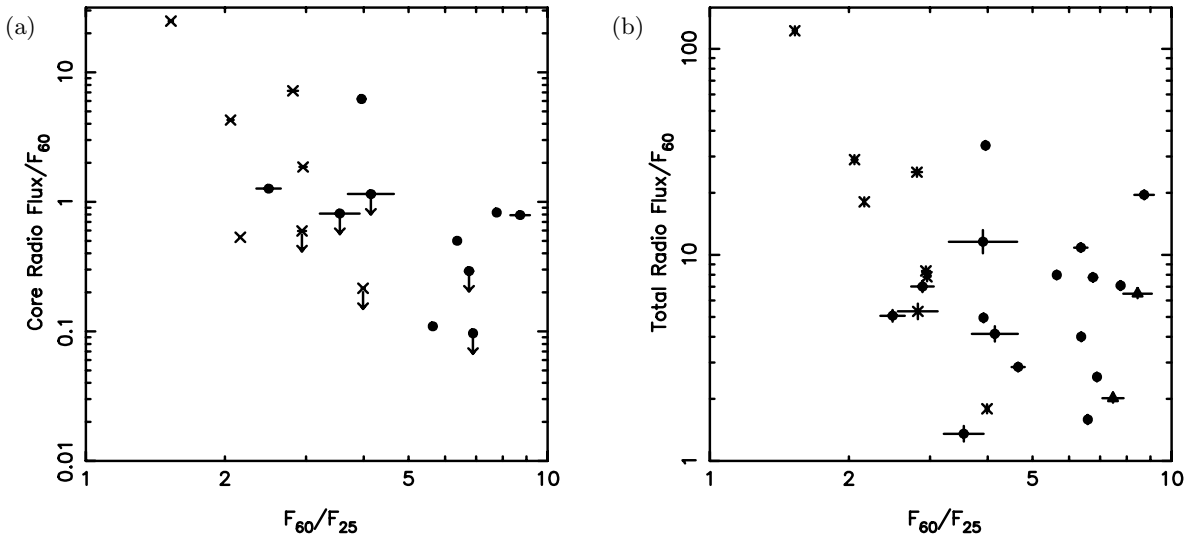

Figure 7: The ratio of (a) core radio flux (essentially an AGN property), and (b) the integrated radio flux, and the 60μm flux. These are both measures of how luminous the central AGN is relative to any star formation present. The first shows a trend for HBLRs to have higher values of the ratio. Since the actual radio luminosities between the HBLRs and non-HBLRs are not significantly different, this shows that the 60μm flux must be larger in the non-HBLRs. The trend is not as obvious in (b) especially if the radio galaxy IC5063 is removed from consideration, showing the integrated radio luminosity is determined in part at least by the total activity present in the galaxy and not just the core. The symbols are as in Figure 3.

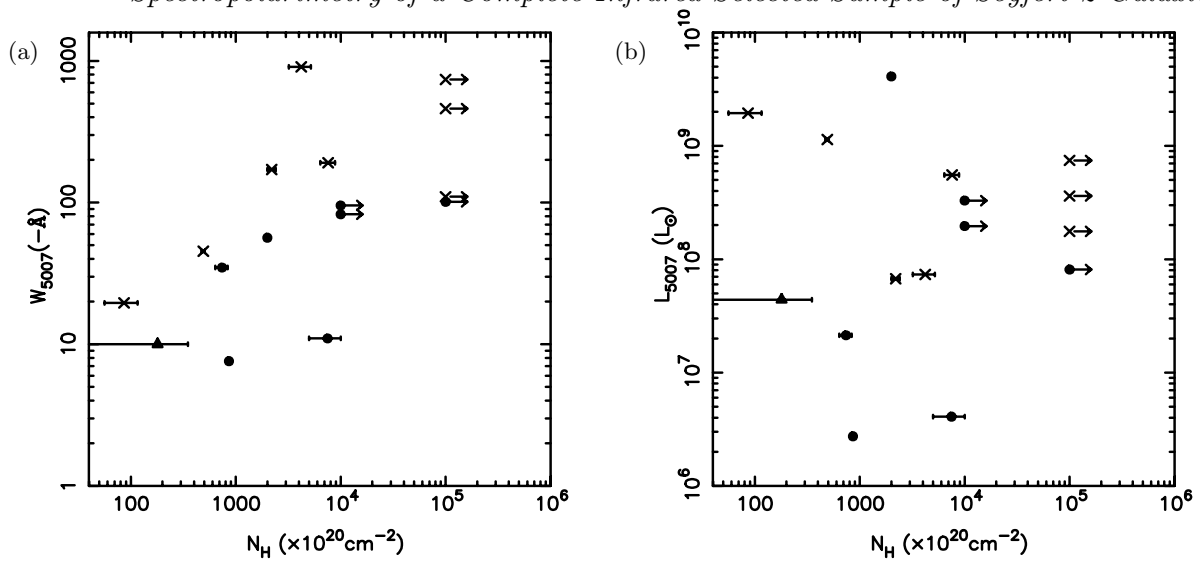

Figure 8: The data in our sample plotted as a function of (a) AGN to host galaxy luminosity and obscuration and (b) AGN luminosity and obscuration. All of the non-HBLRs lie at lower AGN luminosities than the HBLRs at equivalent column densities. This shows how luminosity and obscuration are both important in determining our ability to see an HBLR. The symbols are as in Figure 3.